RELATIVISTIC DYNAMICS AND STRUCTURE FORMATION IN A MATTER—DOMINATED FRIEDMANN UNIVERSE

ROBERT NYAKUNDI NYAGISERA

A Thesis Submitted in Partial Fulfilment for the Requirements of the Award of the Degree of Master of Science in Physics of Masinde Muliro University of Science and Technology

AUGUST, 2024

DECLARATION

This thesis is my original research work prepared with no other than the indicated sources and support and has not been presented elsewhere for a degree or any other award.

Signature:…… Date:…….....

Robert Nyakundi Nyagisera

SPH/G/01–54181/2017

CERTIFICATION

The undersigned certify that they have read and hereby recommend for acceptance of Masinde Muliro University of Science and Technology a Thesis entitled "***Relativistic Dynamics and Structure Formation in a Matter–Dominated Friedmann Universe***"

Signature:…… Date:…….

Dr. Bernard Rapando,

Department of Physics,

Masinde Muliro University of Science and Technology.

Signature:…… Date:.....

Dr. Dismas Wamalwa,

Department of Physical Sciences,

Meru University of Science and Technology.

Signature:…… Date:……..

Dr. Celine Awino Omondi,

Department of Physics,

Masinde Muliro University of Science and Technology.

COPYRIGHT

DEDICATION

This research work is dedicated to my family members, my siblings, Benard Nyagisera and Risper Nyagisera, my mentors Mr. and Mrs. Mogunde and all my beloved friends for their advice, support, encouragement and prayers during my studies.

AKNOWLEDGEMENTS

My kind appreciation goes to the administration of Masinde Muliro University of Science and Technology and the Department of Physics for the support and guidance which contributed to the success of this thesis.

It has been great pleasure to be nurtured by Dr. Dismas Wamalwa Simiyu, Dr. Benard Rapando, and Dr. Celline Awino Omondi over the course of my masters research for their invaluable sacrifices, suggestions, comments, guidance, providing most of literature and being generous with their time that helped make this research a reality. To Prof. Bonface Ndinya, Dr. Henry Barasa and Dr. Maxwell Mageto, the Chairperson Physics Department. I am really grateful for their support.

I will forever be indebted to Dr. Dismas Simiyu for being always present and a dependable supervisor even in times of tight schedule where he sacrificed his official duties to attend my work. He assisted greatly in conceptualization of this research work and was always available for consultation even at odd hours. I thank God for this special gift of life and wish him good health.

Finally, I wish to acknowledge the anonymous reviewers in the Journal of Astronomy for their useful comments that made this work better especially on graphical simulation and general format of this thesis. Their comments, suggestions and opinions contributed to good quality of this thesis.

ABSTRACT

Cosmology as the study of the Universe as a whole, addresses questions on its origin and development and among the unresolved problems in cosmology today is the formation and evolution of structures in the Universe. One of the proposed and successful cosmological model and tested experimentally in addressing this problem is the Friedmann model based on the cosmological principle. This thesis explores the fundamental cosmological principle, with a specific focus on the homogeneity and isotropy assumptions inherent in the Friedmann model underpinning the standard model. The cosmological principle says that the Universe is isotropic and homogeneous on large scales. However, current three-dimensional redshift surveys map the Universe depicting inhomogeneities at all cosmic scales contrary to the cosmological principle view that cosmic matter distribution is statistically isotropic and homogeneous at large length scales. Additionally, there has been an ongoing cosmological debate on whether or not the analyses showing fractal clustering is carried using proper treatment of data, most notably a reliable and accurate amount of available statistical data. These galaxy surveys provide limited statistical data depended on our ability to measure distance accurately. The uncertainties associated with cosmic distance measures are huge and unresolved to date while the availability of huge observational data will wait for the next generation of bigger and advanced telescopes. To address this challenge, the research proposed a modified Friedmann model describing relativistic dynamics, structure formation and evolution based on the distribution of luminous matter in the Universe. In the modified model in which the redshift scale factor relation has been modified, it was assumed that there is huge and accurate astronomical data for measured redshift, number density of galaxies counts per solid angle in a given direction and light intensity counts . Interconnections of these three astronomical quantities was found using Einstein Field Equations. Computer simulations of the derived analytical results produced and the results related to structure formation in a matter–dominated modified Friedmann Universe without dark energy. Galaxy formation, evolution and distribution explained with a modified redshift formalism and compared to the standard model predictions. Analysis of the results suggests that the model can account for cosmic acceleration expansion without the need for dark energy. Simulations based on these models have illuminated structure formation and evolution processes of the early Universe running into the future. The simulations and analytical solutions reveal a unique pattern in the formation and evolution of cosmic structures, particularly in galaxy formation. This pattern shows a significant burst of activity between redshifts $0 < z < 0.4$, which then progresses rapidly until approximately $z \approx 0.9$, indicating that majority of cosmic structures formed during this period. Subsequently, the process slows down considerably, reaching a nearly constant rate until around $z \approx 1.6$, after which a gradual decline begins. There is a distinctive redshift transition around $z \approx 0.9$ is observed before the onset of dark–matter–induced accelerated expansion. This transition is proportional to mass matter density and geometry of the Universe. The model's ability to explain cosmic acceleration without requiring fine-tuning of the cosmological constant highlights its novelty, providing a fresh perspective on the dynamic evolution of the universe.

TABLE OF CONTENTS

LIST OF FIGURES

LIST OF ACRONYMS AND SYMBOLS

$\rho(t)$	Cosmic matter density
λ	Cosmological constant term
$G^{\mu\nu}$	Einstein tensor
$R^{\mu\nu}$	Ricci curvature tensor
S_r	Surface area of a sphere
$T^{\mu\nu}$	Stress–energy/energy–momentum tensor
$g^{\mu\nu}$	Metric tensor
EFE	Einstein Field Equations
FLRW	Friedmann–Lemaitre–Robertson–Walker
I	Intensity of light
IAU	International Astronomical Union
Mpc	Mega parsec
SDSS	Sloan Digital Sky Survey
G	Newton's Gravitational constant
L	Absolute luminosity of star or galaxy
R	Ricci curvature scalar
c	Light speed in a vacuum
$f(z)$	Modified cosmological redshift
k	Cosmic spatial curvature
n	Number density per solid angle
$p(t)$	Cosmic pressure
z	Standard cosmological redshift

CHAPTER ONE
INTRODUCTION

1.1.Background Information

The fundamental aim of modern research in cosmology is to understand large length scale matter distribution and spacetime structure of the Universe from cosmological observations and experimental detection techniques. Many theoretical models explaining the distribution of matter in the matter–dominated Universe have been put forward but there is still some unresolved problems as none of these has satisfactorily explained matter distribution in the Universe (Miguelote & Ribeiro, 1998).

The three dimensional maps of the Universe suggesting a mismatch from traditional held view that matter distribution in the Universe follows homogeneity and isotropy trend on large scale makes this field an open research area that needs further cosmological scrutiny. Whereas the two-dimensional projection obtained by observing the sky shows an averagely isotropic and homogeneous Universe, the three-dimensional catalogues paint a contrasting picture of an inhomogeneous Universe (Conn, *et al*., 2013).

General Relativity, which explains gravity differently from Newton's law set the foundational pillar of modern theoretical cosmology (Einstein, 1915). Einstein's thoughts of General Relativity revolutionized the reflection about the nature of spacetime structures. General Relativity describes the fundamental interaction of gravity caused by spacetime structures being curved by matter and energy using a set of 10 Equations (Einstein, 1915).

Einstein's field equations without dark energy are expressed as (Lahav, 2017):

$$G_{\mu\nu} = R_{\mu\nu} - \frac{1}{2} g_{\mu\nu} R = \beta T_{\mu\nu} \qquad (1.1)$$

where $G_{\mu\nu}$ is the Einstein tensor computed from the metric, $R_{\mu\nu}$ is the Ricci tensor, $g_{\mu\nu}$ is the metric tensor, R is the Ricci scalar, $T_{\mu\nu}$ is the stress–energy (energy–momentum) tensor describing the matter and includes all the sources of matter that can curve spacetime, and

$$\beta = \frac{8\pi G}{C^4} \tag{1.2}$$

with *G* as the Newton's gravitational constant and *c* is the light speed in free space.

The exploration of Einstein's field equations solved in a cosmological setting from a purely theoretical physical law (Einstein, 1917) combined with the findings of Edwin Hubble (1926) led to the emergent of the cosmological principle. As per this principle, the Universe is spatially homogeneous and isotropic when averaged over some large length scale. This homogeneity scale has been evolving in time, from a few mega parsecs (MPc) at initial stages to tens of MPc presently.

Friedmann (1922) discovered a non–static solution of the Einstein's field equations hinting for an expanding Universe (Friedmann, 1922). This was independently supported by (Lemaitre, 1927) who proposed the distance–redshift relationship that would explain cosmic expansion. These discoveried combined with the metric of Robertson and Walker, led to the Friedmann–Lemaitre–Robertson–Walker solution (Friedmann model) of Einstein's field equations of General Relativity and which we view as the best fit model to describe evolution and dynamics of the Universe (Gomez, 2011).

The Friedman model follows the cosmological assumption that the Universe is homogeneous and isotropic at any given cosmic time, t and describes an expanding cosmos. This gives the hyper–surfaces of Einstein Universe to be smooth surfaces with

constant time, t and having a preferred time coordinate, t such that the t = constant slices are homogeneous and isotropic spaces (Wamalwa, 2016). There exists three kinds of hyper─surfaces representing homogenous and isotropic metrics with different large scale geometries: with constant curvature $k=0$ (no curvature) representing the metric of flat space (Euclidean space), with constant curvature $k=+1$ (constant positive curvature) representing the metric of closed sphere space and with constant curvature $k=-1$ (constant negative curvature) representing the metric of open hyperbolic space. The three hyper-surface metric spaces can be combined together uniformly using stereographic projection in rectangular coordinate system on the three-dimensional projection space (Wamalwa, 2016). In case homogeneity or isotropy or both are broken, then the Friedmann model cannot give correct predictions of the Universe (Melia & Shevchuk, 2012). Nevertheless, the history of observational cosmology shows that each time improved instruments permit deeper surveys, the new data reveals inhomogeneous matter distribution on the new scale (Mustapha *et al.*, 1997).

It is claimed that the matter─dominated Universe is model dependent on the description of structure formation and the nature of galaxy distribution in space when on the application of common cosmological statistical techniques. The available statistical galaxy clustering estimation assume that the surveys from which the analysis is made are much larger than the scale of homogeneity. If the current surveys appear below the homogeneity scale, as a close approximation of the main redshift survey, the distribution of galaxy is approximated by a fractal (Amendola & Palladino, 1999).

Presently, there are huge catalogue compilation that lists objects in the sky and their distance from us together with the direction from which their lights reaches us hence, they provide us with a three dimensional pictures of luminous matter in spacetime. These

pictures suggests inhomogeneous distribution of galaxies at smaller and larger distances casting doubt on the cosmological principle view that the Universe is statistically isotropic and homogeneous at large scales. However, two dimensional projection obtained by observing the sky shows an averagely isotropic and homogeneous Universe in contrast to the three-dimensional catalogues that paint an inhomogeneous picture of the Universe (Wamalwa, 2016).

Not long ago (Meszaros, 2019), observed that gamma ray bursts on large length scales of gigaparsecs show a strong contradiction with the cosmological principle, which requires a transition scale of homogeneity below the gigaparsec scale. However, the author acknowledges the limitation of the used data and warns of any premature conclusion to dismiss the cosmological principle. This invokes the question as to whether the Universe is indeed modeled by the Friedmann or fractal distributions.

By fractal, we mean an inhomogeneous structure which is self-similar or exhibiting self-regularity. Given the quantity $N(r)$ as the characteristic of the distribution that exhibit fractal behavior i.e. number of elementary objects (galaxies) and r is the scale measure of dimension length, the mathematical relation takes the form:

$$N(r) = B\, r^{\,D_F} \tag{1.3}$$

where D is the Fractal dimension and is usually assigned integer values such that: D = 0 describes a point distribution, D = 1 indicate that galaxies in roughly linear structures (filaments) describing a linear distribution, D = 2 describing a roughly sheet-like structure distribution describing a surface distribution, and D = 3 describes a uniform distribution (space filling distribution of galaxies) (Mureika, 2007). A homogeneous distribution

Universe manifest at D = 3. Fractal dimension D < 3 indicates that galaxies do not fill space in a homogeneous fashion implying fractal (inhomogeneity).

The standard cosmological model predicts that the fractal dimension should approach the homogeneous value at D = 3 on large enough scales; transiting from inhomogeneity to homogeneity (galaxy distribuiom on small scales is believed to be inhomogeneosu).

It is clear from the afore–going discussion that the observational data from three-dimensional catalogues tend to pose a threat to the validity of the Friedmann model and the cosmological principle in general. However, these galaxy surveys provide only limited statistical data and are depended on our ability to accurately measure redshift as a distance indicator. To understand the large scale structure, we need better quality data beyond 200MPc. The Sloan Digital Sky Survey (SDSS) which is biggest at the moment only surveys a quarter of the sky and gives us data of less than 200MPc (York, *et al*., 2000). Vera Rubin Observatory in Chile with the best camera of 3.6 Gigapixels is expected in 10-years' time to image the entire visible night sky in deep exploration of the entire solar system and into the extragalactic Universe, revealing cosmic explosions and effects of dark matter (Brough, *et al*., 2020).

The uncertainties associated with cosmic distance measures are huge and unresolved to date (Grijs, 2012) while the availability of huge observational data will wait for the next generation of bigger and advanced telescopes (Langa *et al*., 2017). In contrast to Langa *et al*., (2017), we have modified the redshift relation to account for any unknown astrophysical effects. Therefore, the modified redshift relation departs from the standard redshift paradigm; a distinctive signature of this work.

Distance to celestial objects is one of the key astrophysical parameters. There are a variety of distance estimation methods to celestial objects based on geometrical, semi-

geometrical, photometric and kinematics. Each technique has limited range of practical use, such as the radar technique for solar system objects, parallax methods for stars on the range of a few kilo parsec (kpc), Cepheid standard candles to a few Mega parsec and Type Ia Supernovae to several 1000 Mega parsec. Each method above which makes a step in the distance ladder is used to calibrate the next most distant method. Beyond the distances which can be reached using the geometrical or semi-geometrical techniques, objects with known luminosities are also adopted (Smith *et al.*, 2017). They include Cepheids, RR Lyrae, Mira stars and Red Clump (RC) stars. Type Ia Supernovae are standardizable candles as their luminosities are not known, but a specific relationship between their brightness and the time it takes for them to decay exist. Bright Supernovae are known to shine longer than faint Supernovae intrinsically (Humay *et al.*, 1995).

This thesis sought for appropriate cosmological model to accurately describe luminous matter distribution in the Universe. Ultimately, as more data is gathered about distant galaxies, such cosmic measurements should become even more accurate, and physicists may be able to distinguish better the competing cosmological models (Werner & Schermelleh, 2010). This problem was approached by closely following the procedure adopted by Langa *et al*., (2017).

1.2 Statement of the Problem

The Friedmann model based on the cosmological principle is the cornerstone of modern cosmology. The theory has successfully described structure formation and evolution in the Universe in agreement with most observations. Nevertheless, as the various three–dimensional redshift surveys probe in depth into the Universe, they tend to uncover inhomogeneous structures with no transition to homogeneity. These evidences suggests a

violation of the cosmological principle and challenges our understanding of the Universe. However, there has been an ongoing cosmological debate on whether or not the analyses showing inhomogeneity have been carried using accurate and reliable observational data. These theories basing on the contention that the redshift as a common distance indicator at cosmological scales might be biased or inconsistent hint that the standard cosmological theories (Friedmann model) might not be fully accurate reinforcing the modification of the standard redshift relation. In addition to the shift from the Friedmann model, these galaxy surveys provide only limited statistical data depended on our ability to measure redshift as a distance relation accurately. The uncertainties associated with cosmic distance measures are huge and unresolved to date while the availability of huge and accurate observational data will wait for the next generation of advanced astronomical equipment. Therefore, the Friedmann model adopted in the description of luminous matter distribution in the Universe suffers lack of cosmological accuracy. Consequently, structure formation predicted by this model may not be an accurate picture of the Universe. This research proposed a modified Friedmann model by modifying the standard redshift relation for photons in order to describe relativistic dynamics, structure formation and evolution based on the distribution of luminous matters in the Universe. This model avoids the cosmological constant problem, explains the cosmic accelerating Universe in both light intensity, number density of galaxies (or stars), and provides a very natural way to solve the coincidence problem. Therefore, assuming there are huge, consistent and accurate astronomical data for measured redshift, number density counts of galaxies per solid angle in a given direction and light intensity counts of galaxies, interconnections of these three astronomical quantities has been determined using Einstein field equations and related them to structure formation in a matter–dominated modified Friedmann Universe.

1.3 Objectives

1.3.1 Main Objective

To study the relativistic dynamics and structure formation of luminous matter distribution based on a modified redshift relation in a matter-dominated Friedmann Universe.

1.3.2 Specific Objectives

1. To derive Friedmann Equations governing dynamics of the Universe within Einstein Theory of General Relativity considering isotropy and homogenity.
2. To formulate a modified redshift relation in the classical equation between cosmological redshift and cosmic scale factor for photons within Einstein Theory of General Relativity.
3. To derive light intensity and number density relations with modified redshift using Friedmann Equations.
4. To explain the implications of the modified redshift on structure formation in a matter−dominated Friedmann Universe.

1.4 Justification

Astronomical studies are very crucial as they are the cornerstone in describing matter distribution in the Universe. The Friedmann model based on the cosmological principle has successfully described structure formation in the Universe is therefore the integral life of astrophysicists so that the presence of large−scale inhomogeneity in matter distribution against the cosmological principle supporting a homogeneous Universe will appear revolutionary not only physics but also science in general. Presence of cosmic inhomogeneities can provide an alternative explanation of global cosmic acceleration without an additional dark energy. This research will also put us in a position to test

whether or not luminous matters in the universe are homogeneously or obey fractally systems distribution at large scales.

1.5 Significance

The cosmological principle is key to the formation of the standard cosmological model, which gives the insights of the dynamics of the Universe. This study is of great significance as it will help challenge the existing standard model of cosmology and shift the focus to a modified Friedmann model in predicting the future and fate of the Universe. With the achievement of the stated objectives, we will be at a better position to describe distribution of luminous matter in the Universe and construct the cosmic history of structure formation different from the standard model predictions enabling cosmologists ascertain whether there is a possible paradigm shift in cosmology and as to whether introduction of new Physics knowledge is required.

CHAPTER TWO
LITERATURE REVIEW

2.1 Friedmann Model

The study of the origin and evolution of the Universe is one of the fundamental open questions of modern cosmology. Modern cosmology is an active theoretical and experimental field built systematically, with new problems arising at each step, the theory has to be added new elements in order to explain the arising problems. Some of the current main projects of theoretical physics have something to do with cosmology, whose unresolved problems have motivated many published papers. This justifies the need for understanding the origin of modern cosmology whose theory, observations and experiments are basis of research nowadays (Gomez, 2011).

The idea of Einstein set the pace–study of modern theoretical cosmology. Einstein's paper (Einstein, 1917) inspired new vision of the whole structure of the Universe based on the geometrical point of view of gravity, different from the traditional view of gravity as a force from which a small group of theoretical physicists started advancing their relativistic dynamics cosmological research models based on the new theory of gravitation.

Friedmann (Friedmann, 1922) published dynamic solutions to Einstein's field equations confirming an expanding Universe. By retaining the cosmological principle assumption of a mathematically homogeneous and isotropic four–dimensional cosmos through varying the radius of curvature, *R*, he discovered a dynamic and expanding Universe. Lemaitre (Lemaitre, 1927), while scrutinizing Einstein's fundamental general relativistic equations and supported by cosmological observational evidence (Hubble, 1926), concluded that the Universe is expanding. Later, Einstein agreed to the claim of a dynamic and expanding Universe, refuting his static Universe model on realizing that it was

unstable, and could admit dynamic solutions. This confirmed that the Universe is not only homogeneous and isotropic on large scale but also expanding (Einstein, 1931).

Friedman–Robertson–Walker cosmological model is the widely accepted standard model in describing the Universe and acts as a door opener for researchers to form other different types of cosmological models in describing the Universe (Mohajan, 2013) (hereafter referred as Friedmann model). Ever since the earliest cosmological models, the Einstein and de Sitter models researchers have been trying to fit observations to the Friedmann spatially homogeneous and isotropic family models (Mustapha *et al.*, 1997). The success of reproducing a Hubble redshift-distance (Hubble, 1926) have convinced physicists of its validity as a large length scale description of the Universe. In approximating the realistic description of our actual universe, this model is regarded as a good fit universally (Bolejko *et al.*, 2011).

The cosmological models based on the cosmological principle have had significant successes in explaining observational facts and in anticipating new discoveries. Two successes that rise above all is the prediction of the cosmic microwave background (CMB) which is the electromagnetic radiation that remained after Big Bang and the explanation of the cosmic abundance of light elements (Alpher, 2014). The CMB radiation acts as a powerful tool in investigating the early universe as the information obtained in it is used in constraining the standard cosmological parameters.

Other theories shifting from the standard Friedmann model anchor on the contention that the redshift relation as a distance indicator at cosmological scales might be biased or inconsistent (Shamir, 2024). By cosmological redshift it means wavelength of light is

stretched (or photons lose energy) by cosmic expansion and light is seen as shifted towards the red part of the spectrum.

If the redshift scale factor as a distance indicator is complete and fully accurate, the standard cosmological theories are incomplete. Similarly, if the standard Friedmann model is complete, it is not possible that the distance indicators currently used are fully accurate. International Astronomical Union (IAU) Symposium 289 addressed the physics researches underlying methods of distance determination across the Universe, exploring the various techniques employed and acknowledged the controversy that exist not yet resolved, and that all the techniques applied to date suffer by their own unique set of uncertainties (Grijs, 2012). The assumption is that this problem can only be resolved with immense and direct observational data that does not have distance measurement uncertainties in them. With that, we may be in a position to judge whether, the luminous matter distribution in the Universe follows Friedmann model or not (Langa *et al.*, 2017). Other studies carried out so far on different galaxy surveys claim to have found a transition to homogeneity on sufficiently large scales 70–100 h^{-1}Mpc (Pandey & Sarkar, 2016) whereas some studies claim absence of any such transition out to scale of the survey (Labini, 2011). The results from these studies clearly indicate that there is no definite answer on this issue (Labini, 2011). Therefore, there is a lot of concern to both observational and theoretical cosmologists that the present model may be incomplete or inaccurate. This concern has shifted the focus to thorough scrutiny through research on whether the current Friedmann model is incorrect and if so then what will be its implications in cosmology.

2.2 Fractal Model

A fractal is a self-similar structure. The notion of fractal structures of matter distribution in the Universe from a mathematical view point is associated with power law functions for which the most suitable property is the exponential function; where the amplitude provided by the mathematical relation Equation is a connection with the lower cut−offs of the distribution (Pietronero & Labini, 1996).

Several statistical analyses of three-dimensional galaxy catalogues indicates that galaxy distribution is distributed fractally with dimension $D \cong 2$ out to the largest scales for which statistically significant data is available, i.e., up to about $100-200h^{-1}$Mpc. These theories claim that no data is pointing convincingly towards a homogenization of galaxy distribution (i.e., $D \cong 3$) (Durrer & Labini, 1998).

The first inhomogeneous model proposed by Lambert (1750) involved a ring of stars rotating around a central obscure body, perhaps part of a system of rings rotating around another body. Another inhomogeneous model proposed almost at the same time involving a distribution of radially decreasing worlds (galaxies). The wave evolution goes from inside to outside: while the worlds near the center are already in an advanced stage of evolution, and will disappear first, those near the outer boundary are still in the primordial chaos (Amendola, 1998).

In 1820, Hienrich Olbers presented the well-known Olbers' paradox, already formulated by Halley in 1721 and stated that: any homogeneous, static and infinite model should be in equilibrium everywhere at the temperature of the star's surface. However, clearly, this is not true, because at night, the sky is dark suggesting that the Universe is either not homogeneous or static or the light at the sky has different properties than those we experiment on Earth. For instance, the flux of light we experience on Earth reduces faster

than the distance square law (Amendola, 1998). The possibility of the sky inducing the rotation property in bodies is an evidence that the sky might have different properties than those experienced on earth; a ray of polarized light, along the lines of magnetic force suffer rotation. The non–reversibility of light in a magnetic medium is also in a rotatory motion independent of light propagating through it. Finally, the influences of optical properties of the sky may also change the rules of geometry at larger distances in the sky than those on earth.

Charlie (1908) proposed a hierarchical model with the stars arranged in such a way that their density as seen from any other star decreases with distance. This model regarded as the first fractal model since in this model, the density decreases radially from every star as seen from any star.

The isotropy observed in deeper sky maps is consistent with a Universe that is inhomogeneous but spherically symmetric about our earthly position (Peebles, 1998). This seems to cast doubt to the validity of the cosmological principle.

Critical voices in physics claim that the distribution of matter in the Universe is intrinsically inhomogeneous from the smallest to the largest observed scales and, perhaps, indefinite (Ribeiro & Miguelote, 1998). This notion that galaxies are fractally distributed has been a long-standing hot debate in modern cosmology (Durrer & Labini, 1998).

The recent galactic redshift surveys showing a very inhomogeneous map for the distribution of galaxies have stimulated the trend of study of the galactic clustering problem which assumes that the large scale structure of the Universe can be described as being a self-similar (fractal) system (Ribeiro, 1993).

The quasars are the brightest classes of objects in the Universe called Active Galactic Nuclei (AGN). They are highly luminous enabling them to be detected out at larger length scales. The presence of large quasar groups (LQG) in the quasar distribution (Clowes, *et al.*, 2013) with characteristic size of up to ~500 h^{-1}Mpc at z ~1.3 in the DR7 quasar catalogue and claimed that this structure is incompatible with homogeneity at large length scale showing possible violation of the cosmological principle (Pandey & Sarkar, 2016).

The complete Sloan Digital Sky Survey (SDSS) quasi-stellar object (QSO) that maps the Universe provides a complete sample that covers only a quarter of the observable Universe using clustering statistics (Smith *et al.*, 2017). This volume-limited samples for galaxy clustering statistics are in good agreement with many previous sample analysis, confirming in particular that the galaxy distribution is well defined by a fractal dimension $D \cong 2$ up to a scale of at least 20 h^{-1}Mpc implying a trend towards inhomogeneity (Joyce *et al.*, 2005).

Studies incorporating gamma ray bursts have yielded results that cast doubt on the cosmological principle. Although the large scale average of the visible parts of the Universe appear isotropic and homogeneous in line with the cosmological principle, gamma ray bursts are not isotropic on the sky (Meszaros, 2019).

Availability of huge amount of observational data for better statistical analysis of the large-scale structure of the Universe to determine whether the Universe is compatible with fractal scaling of galactic clustering or not has currently been acknowledged by a fractal researcher who warns scientists on hurried dismissal of the cosmological principle (Meszaros, 2019).

To understand the large-scale structure, it is important to focus our research on the trend of clustering with scale of better data much beyond 200 Mpc although the current Sloan Digital Sky Survey (SDSS) data is about 200 Mpc. The SDSS, which gives approximately a quarter of the sky, is the greatest and most high precision galaxy redshift survey (York, *et al*., 2000) now. The current Vera Rubin Observatory in Chile with the best camera of 3.6 Gigapixels is expected in 10−years' time to image the entire visible night sky in deep exploration of the entire solar system and into the extragalactic Universe, revealing cosmic explosions and effects of dark matter (Brough, *et al*., 2020).

The observed inhomogeneities pose a fundamental challenge to the standard picture of modern cosmology. It has been claimed that this inhomogeneities that extend up to the present large scale observational limits point to a fractal Universe in which structures at small scales get replicated at larger scales (Secrest, *et al*., 2021).

The presence of inhomogeneities or fractality of the Universe on very large scales has several important consequences to our understanding of many physical quantities as defined in the realm of General Relativity. Inhomogeneities can provide an alternative explanation of global cosmic acceleration without requiring an additional dark energy component (Ellis, 2011). This motivates us to establish the validity of the cosmological principle and the standard theory of cosmology in general that is integral part of this work. However, to do this, the research need huge (unlimited) accurate experimental data that is beyond our present technology that do not have assumptions due to distance measure: even the largest Sloan Digital Sky Survey (SDSS) covers only a tiny fraction of the sky (Paris, *et al*., 2017).

The three-dimensional catalogues list astronomical objects in the sky and give their distance away from us together with the direction from which their light reaches us. These three-dimensional pictures reveal an inhomogeneous distribution of galaxies at smaller and larger distances contrary to the cosmological view that the Universe is statistically isotropic and homogeneous at large scales ($> 50\mathrm{Mpc}$) (Labini *et al*., 1998). To address this challenge, we proposed a modified Friedmann model that describing relativistic dynamics, structure formation and evolution based on the distribution of luminous matter in the Universe.

Current observations, such as the unexplained Hubble parameter tensions and large-scale anisotropies, pose challenges to the standard Friedmann model and the concordance model of cosmology in general. For example, the Hubble parameter determined from the cosmic microwave background (CMB) radiation differs from that determined using Type Ia supernovae and the redshift of their host galaxies (Seshavatharam & Lakshminarayana, 2023). Introduction of a new element into the standard model of cosmological may be a key relieving Hubble tension. The possible solution to the Hubble constant problem lies in modification of scale factor evolution before recombination (Kuzmichev & Kuzmichev, 2024).

Given the unsettling findings discussed above, there is a widespread unease regarding the validity of current cosmological models. The research explored the contention on whether the current Friedmann model is consistent, reliable, inaccurate or incomplete through a modified redshift approach and explained the implications of the modified redshift on structure formation in a matter-dominated Friedmann Universe.

CHAPTER THREE
MATERIALS AND METHODS

3.1. Einstein Field Equations

The Einstein Field Equations Equation (1.1) which gives a relation between Einstein tensor and energy–momentum tensor that describes the total energy content of the Universe, all put together gives the dynamics and evolution of the background Universe.

3.1.1. Friedmann–Lemaitre-Robertson–Walker (FLRW) Metric

The FLRW cosmological model (Friedmann model) governs the Universe. The Friedmann model made an intelligent prediction in cosmology about the Universe as early as 10^{-43} seconds after the Big Bang. According to the Friedmann model, cosmological principle is valid and forms the basis of the standard model of cosmology. It assumes that the space is filled by a homogeneous and isotropic matter on large length scales and is described by the following general metric of the functional form:

$$c^2dt^2 - \frac{R(t)^2}{(1+kr^2)^2}\, dr^2 \qquad (3.1)$$

where $dr^2 = dx^2 + dy^2 + dz^2$ and $R(t)$ is the expansion scale factor representing the time–dependent evolution of spatial part of the metric (surfaces of constant time, t) and k = (–1, +1, 0) determines the geometry of these spatial sections: Open, Closed and Flat Universes respectively. Equation (3.1) is the cosmological spacetime metric describing an isotropic, homogeneous and cosmologically expanding cosmos.

The rank 2 covariant metric tensor $g_{\mu\nu}$ is obtained as

$$g_{\mu\nu} = \begin{pmatrix} c^2 & 0 & 0 & 0 \\ 0 & \frac{-R^2(t)}{(1+kr^2)^2} & 0 & 0 \\ 0 & 0 & \frac{-R^2(t)}{(1+kr^2)^2} & 0 \\ 0 & 0 & 0 & \frac{-R^2(t)}{(1+kr^2)^2} \end{pmatrix} \tag{3.2}$$

The FLRW metric can be written as

$$ds^2 = c^2dt^2 - \frac{R^2(t)}{(1+kr^2)^2}\, dr^2 \tag{3.3}$$

From Equation (3.3),

$$g_{00} = c^2 \tag{3.4}$$

$$g_{11} = g_{22} = g_{33} = -\frac{R^2(t)}{(1+kr^2)^2} \tag{3.5}$$

This implies that

$$g^{00} = \frac{1}{c^2} \tag{3.6}$$

and

$$g^{11} = g^{22} = g^{33} = -\frac{(1+kr^2)^2}{R(t)^2} \tag{3.7}$$

Now curvature scalar and components of the Ricci tensor are needed.

Consider the non−vanishing values of the Ricci curvature tensor, R_{00}, R_{11} R_{22} and R_{33} respectively as computed (Wamalwa, 2016) in the form:

$$R_{00} = -\frac{3R''(t)}{R(t)} \tag{3.8}$$

$$R_0^0 = -\frac{3R''(t)}{C^2R(t)} \tag{3.9}$$

$$R^{00} = -\frac{3R''(t)}{c^4R(t)} \tag{3.10}$$

and also

$$R_{11} = R_{22} = R_{33} = \frac{R(t)\,R''(t) + 2\,R'(t)^2 + 8kc^2}{c^2\,(1+kr^2)^2} \tag{3.11}$$

$$R_1^1 = R_2^2 = R_3^3 = \frac{R(t)\,R''(t) + 2\,R'(t)^2 + 8kc^2}{c^2\,R(t)^2} \tag{3.12}$$

$$R^{11} = R^{22} = R^{33} = \frac{8kc^2 + R(t)R''(t) + 2\,R'(t)^2}{c^2\,R(t)^4}\,(1 + kr^2)^2 \tag{3.13}$$

The Ricci curvature scalar is written as

$$R = R_u^u = (R_0^0 + R_1^1 + R_2^2 + R_3^3) \tag{3.14}$$

So that on using Equation (3.9) and Equation (3.12) into Equation (3.14) gives the Ricci curvature scalar as

$$\mathrm{R} = R_u^u = -\frac{3\,(8\,kc^2 + 2\,R(t)R''(t) + 2R'(t)^2)}{c^2R(t)^2} \tag{3.15}$$

The energy-momentum tensor also has components computed as (Wamalwa, 2016)

$$T^{00} = \rho(t) \tag{3.16}$$

and

$$T^{11} = T^{22} = T^{33} = \frac{(1+kr^2)^2}{R(t)^2} P(t) \tag{3.17}$$

where $\rho(t)$ and $P(t)$ is the mass density and pressure of the Universe respectively.

In order to describe the relativistsic dynamics and evolution of the cosmos, consider the contravariant forms of the Einstein Field Equations (1.1)

$$G^{\mu v} = R^{\mu v} - \frac{1}{2} R g^{\mu \nu} = \beta\, T^{\mu \nu} \tag{3.18}$$

In the next chapter, Equation (3.18) will yield specific Einstein Field Equations for describing dynamics and evolution in the matter−dominated Friedmann cosmology.

3.2 A Modified Redshift Relation for Light Photons

The classical relation between cosmological redshift and cosmic scale factor for photons is expressed as (Langa *et al*., 2017)

$$1 + z = \frac{R(t_0)}{R(t_e)} \tag{3.19}$$

where $R(t_e)$ is the cosmic scale factor at the time of photon emission, $R(t_0)$ is the cosmic scale factor at the time of photon observation and z is the cosmological redshift. The relation in Equation (3.19) is herein referred as the standard redshift relation. Should we posit that unknown quantum effects exert a discernible influence on the frequency of light photons during their cosmological propagation, but the time dilation of two macroscopic events caused by cosmic expansion will not be affected, the aforementioned relation can be modified to

$$1 + f(z) = \frac{R(t_0)}{R(t_e)} \tag{3.20}$$

where $f(z)$ is the modified model redshift.

In contrast to earlier works (Langa *et al*., 2017), the standard redshift relation has been modified and the relativistic dynamics and structure formation in the matter–dominated Friedmann Universe has been explored in the absence of dark energy. In this modified model, because of the modification of the redshift relation for photons, cosmic history of luminous matter distribution at any cosmic time deviates from the prediction of the standard matter–dominated Universe providing a very natural way to solve the coincidence problem. This feature also exists in the models with Tolman's dimming of light. In the relativistic dynamic evolution of the Universe, we do not need the vacuum energy. This mechanism make quantum vacuum contribute nothing to gravitational pull and has been used to solve the cosmological constant problem. The modified redshift considered here is more generic and account for any unknown astrophysical effects in the Universe not revealed by the standard model.

The redshift Equation of photons Equation (3.19) may not be accurate enough to describe dynamics and evolution of the Universe. This type of modification proposed by (Tian, 2017) yielded good results and is therefore not far-fetched.

The above redshift modification considered with the matter–dominated Friedmann Universe has explained the dynamics in the accelerating expansion of the late time Universe.

It is clear from the modified redshift Equation that if $f(z) = z$, then the modified model recovers the standard redshift Equation in its usual form.

3.3 Variation of Light Intensity and Number Density with Modified Redshift

We assumed to be given huge and direct observational data of the following astronomical quantities that have no assumptions about the background geometry or uncertainties in distance measurements:

(i) Light intensity (I) from an astronomical object e.g., a star or galaxy

(ii) Redshift z of the light intensity from the given astronomical object in (i) above in a given direction

(iii)The number density (n) per solid angle of a class of objects in a given direction.

In order to derive a relation between light–intensity and redshift parameter at the beginning of light photon (emission) to the end of light photon (observation), suppose that an astronomical object such as a star or galaxy emits light at $r(t_e)$ and travels towards the origin of our coordinate system such that at time $t = t_0$, it is observed at the origin $(r(t_0) = 0)$.

For null geodesics, ds = 0, from Equation (3.3) expressed as

$$\frac{c}{R(t)}dt = -\frac{1}{1+kr^2}\,dr \qquad (3.21)$$

where we have assumed that dt is positive and dr is negative (application of the principle of reversibility of light). Performing integration of Equation (3.21) from time of emission $r(t_e)$, (t_e) to observation time $r(t_0)$, (t_0)), the Equation is expressed as

$$\int_{t_e}^{t_0}\frac{c}{R(t)}dt = -\int_{r(t_e)}^{r(t_0)}\frac{1}{1+kr^2}\,dr \qquad (3.22)$$

Here, dr is the comoving distance that photons travel at time dt. Equation (3.22) is the general Equation for describing dynamics and evolution of the Universe. In the next chapter, a solution for dr is derived based on this Equation for different geometry of the Universe. Combining this solution with derived results of Einstein Field Equations in view of the modified redshift Equation (3.20), a general analytical solution on how light intensity and number density of galaxies vary with modified redshift has been formulated for describing dynamics, structure formation and evolution of observable Universe.

3.4 Assumptions

It is assumed that the astronomical objects (stars or galaxies) under considerations are distributed uniformly in the Universe such that you can count the number of stars you observe in a given redshift.

In addition, the Universe's matter content must be a perfect fluid as a necessary and sufficient condition for spacetime to satisfy the FLRW model. Meaning that its velocity field source should have no rotation, shear and acceleration.

3.5 Software use for Result Analysis

This section gives the procedure of simulating the predictions derived from the analytical results; the Equations governing light intensity and number density for the modified Friedmann model. The parameter values employed in these simulations are meticulously chosen, with constraints derived from cosmological observational data. Variations in parameters achieved through a nuanced adjustment in the MATLAB application and shed light on the kind of universe expected from the model when MATLAB version R2017b (MathWorks-Inc., 2017) simulations are run in the background. There are subtle variation in parameters and serves the dual purpose of exploring additional statistically significant features of cosmic structures revealing the resilience of the model under slight perturbations and for comparison under consistent matter density and curvature of the universe.

All values employed in the codes adhere to existing statistical data. To examine the initial effects of cosmic acceleration on galaxy formation in both models, the number density curves are individually plotted first. The same procedure is applied for graphing light intensity analytical result. To evaluate the impact of introducing the modified model in the cosmic background, both the standard redshift and modified redshift models without dark energy are plotted on the same scale for comparison.

CHAPTER FOUR
THEORETICAL FRAMEWORK

4.1 The Governing Equations

4.1.1 Einstein Field Equations

Einstein Field Equations relates the total energy contents of the Universe with its curvature. So according to Einstein Field Equations (1.1), the left–hand side dictates how matter and energy curve spacetime and the right hand side tells matter and energy how to move through a curved spacetime as introduced in chapter one.

4.1.1.2 Einstein Tensor Components

The zero–zero Einstein tensor components are computed as follows.

Setting μ, ν = 0, Equation (3.18) becomes

$$G^{00} = R^{00} - \frac{1}{2}Rg^{00} = \beta T^{00} \tag{4.1}$$

4.1.1.3 First Friedmann Equation

By putting all the necessary pieces in one place by substituting Equations (3.6), (3.10), (3.15) and (3.16) into Equation (4.1), to get the Einstein Equation.

$$G^{00} = -\frac{3R''(t)}{c^4R(t)} + \frac{3\,(4\,kc^2 + R(t)R''(t) + R'(t)^2)}{c^4R(t)} = \beta\rho\,(t)$$

$$= -\frac{3R''(t)\,R(t)}{c^4R(t)^2} + \frac{12\,kc^2 + 3\,R'(t)^2)}{c^4R\,(t)^2} + \frac{3R''(t)R(t)}{c^4R(t)^2} = \beta\rho\,(t)$$

$$\Rightarrow 12\,kc^2 + 3R'(t)^2 = \beta c^4R(t)^2\rho\,(t) \tag{4.2}$$

4.1.1.4 Second Friedmann Equation

To calculate the second Einstein Equation, set $\mu = \nu = 1, 2, 3$ in Equation (3.18) as

$$G^{11}=G^{22}=G^{33}= R^{11}— \frac{1}{2}Rg^{11}=\beta\, T^{11} \tag{4.3}$$

Substituting Equations (3.6), (3.10), (3.15) and (3.16) into Equation (4.3) to get

$$G^{11} = \frac{8\,kc^2+ R(t)R''(t)\ +2\,R'(t)^2)}{c^2R(t)^4} — \frac{(12\,kc^2+ 3\,R(t)R''(t) + 3\,R'(t)^2)}{c^2R(t)^4} = \frac{\beta P(t)}{R(t)^2}$$

$$= \frac{-4\,kc^2- 2\,R(t)R''(t) - R'(t)^2)}{c^2R(t)^2} =\beta P(t)$$

$$\Rightarrow\ 4\,kc^2 + 2\,R(t)R''(t) + R'(t)^2 = —\ \beta c^{\,2}R(t)^2P(t) \tag{4.4}$$

Equations (4.2) and (4.4) are the first and second specifc Friedmann Equations for describing dynamics and evolution of the Universe.

In the next section, a conservation law is developed based on Equations (4.2) and (4.4) paying special attention to conserved observables enabling formulation of a general analytical solution.

4.1.2 Energy Conservation law

Differentiating Equation (4.2) with respect to t gives

$$6\,R'(t)R''(t)= 2\beta c^4R(t)R'(t)\rho\,(t) + \beta\,c^4R(t)^2\rho'(t) \tag{4.5}$$

where $R''(t) = \frac{d\,R'(t)}{dt}$ and $R'(t) = \frac{d\,R(t)}{dt}$. Multiplying the result above by $R(t)$ gives

$$6R(t)R'(t)R''(t)= 2\beta c^4R(t)^2\,R'(t)\rho(t) + \beta\,c^4R(t)^3\rho'(t) \tag{4.6}$$

Lets now multiply Equation (4.4) by 3 to give

$$12kc^2 + 6R(t)R''(t) + 3\,R'(t)^2 = -3\beta c^2 R(t)^2 P(t)$$

Scalar multiplication to solutions of homogeneous differential Equations is also a solution. Re-organizing this Equation yields

$$6R(t)R''(t) = -(12kc^2 + 3R'(t)^2) - 3\beta c^2 R(t)^2 P(t) \qquad (4.7)$$

Applying Equation (4.2) into Equation (4.7) to obtain

$$6R(t)R''(t) = -\beta c^4 R(t)^2 \rho(t) - 3\beta c^2 R(t)^2 P(t)$$

Multiplying this result by $R'(t)$ gives

$$6\,R(t)R'(t)R''(t) = -\beta c^4 R'(t)R(t)^2 \rho(t) - 3\beta c^2 R'(t)R(t)^2 P(t) \qquad (4.8)$$

Subtracting Equation (4.8) from Equation (4.6), gives

$$3c^2 R'(t)\mathrm{R}(t)^2 \rho(t) + c^2 R(t)^3 \rho'(t) = -3R'(t)R(t)^2 P(t)$$

Lets rewrite this result to read as

$$\frac{d}{dt}(c^2 \rho(t) R(t)^3) = -P(t)\frac{d}{dt}R(t)^3 \qquad (4.9)$$

Equation on the left–hand–side represent the rate of change of total energy in the Universe while the right–hand–side is the work it does as it expands ($-Pdv$). The case of interest is the matter–dominated cosmology. In the matter–dominated cosmology, the main energy density of the cosmological fluid is in cold non–relativistic matter particles which behave like dust: $P = 0$, so Equation (4.9) becomes

$$\frac{d}{dt}(c^2\rho(t)\mathrm{R}(t)^3) = \text{constant}$$

$$\Rightarrow \rho(t)\mathrm{R}(t)^3 = \text{constant, } \alpha \qquad (4.10)$$

Equation (4.10) represents the conservation law for the stress–energy momentum tensor for a matter–dominated Universe. It says that the total mass contained in the Universe remains constant. This shows that the total matter content in the Universe remains constant at any given time and therefore, Equation (4.10) describes a matter dominated Friedmann Universe. This is in line with the relativistic theory of matter and fields (Noether's theorem) in which there is no preferred direction for motion of matter, otherwise isotropy would be broken.

Rewrite Equation (4.2) to read as

$$12kc^2 + 3R'(t)^2 = \frac{\beta\, c^4 R(t)^3 \rho(t)}{R(t)}$$

So that upon using Equation (4.10) in this result yields

$$12\, kc^2 + \, 3\, R'\,(t)^2 = \frac{\beta\, \alpha\, c^4}{R(t)} \qquad (4.11)$$

Dividing Equation (4.11) by 3 on both sides gives

$$4\, kc^2 + R'(t)^2 = \frac{\beta\, \alpha\, c^4}{3\, R(t)} \qquad (4.12)$$

Making $R'(\mathrm{t})$ the subject of the formula and rearranging the Equation give

$$R'(\mathrm{t}) = \sqrt{\frac{\beta c^4 \alpha}{3\,R(t)} - 4\,kc^2}$$

Which can also be expressed as

$$\frac{dR}{dt} = \sqrt{\frac{\beta\ c^4\ \alpha}{3\ R(t)} -\ 4\ kc^2}$$

$$\Rightarrow dt = \frac{dR}{\sqrt{\frac{\beta\ c^4\ \alpha}{3\ R(t)} - 4\ kc^2}} \tag{4.13}$$

Equation (4.13) is the time taken for a light photon to travel at a distance dr.

4.2 Light intensity–Modified Redshift Relation

Lets explore to derive a relation between light–intensity and redshift parameter at the beginning of photon (emission) to the end of photon (observation).

Consider Equation (3.22) and lets solve this Equation for the comoving distance dr that a photon travels at a time dt. Substituting Equation (4.13) into Equation (3.22) give

$$\int_{R(t_e)}^{R(t_0)} \frac{c\ dR}{\sqrt{\frac{\beta\ c^4 \alpha R(t)^2}{3\ R(t)} - 4\ kc^2 R(t)^2}} = -\int_{r(t_e)}^{r(t_0)} \frac{1}{1+kr^2}\ dr$$

$$\Rightarrow \int_{R(t_e)}^{R(t_0)} \frac{dR}{\sqrt{R}\sqrt{\frac{\beta\ c^2 \alpha}{3} - 4\ k\ R(t)}} = -\int_{r(t_e)}^{r(t_0)} \frac{1}{1+kr^2}\ dr \tag{4.14}$$

Equation (4.14) is the general Friedman Equation for describing dynamics and evolution of the matter–dominated Universe. In the following section, Equation (4.14) has a solution for three different curvature scalars of the Universe: $k = (-1, 0, +1)$, which stand for Open Universe, Flat Universe and Closed Universe respectively.

4.2.1 Flat Universe

Setting $k = 0$, Equation (4.14) becomes

$$— \int_{r(t_e)}^{r(t_0)} dr = \int_{R(t_e)}^{R(t_0)} \frac{dR}{\sqrt{R}\sqrt{\frac{\beta c^2 \alpha}{3}}} = \int_{R(t_e)}^{R(t_0)} \frac{R^{-\frac{1}{2}}\, dR}{\sqrt{\frac{\beta\, c^2\, \alpha}{3}}}$$

This Equation is integrated as

$$r(t_e) — r(t_0) = \frac{1}{\sqrt{\frac{\beta\, c^2\, \alpha}{3}}} \int_{R(t_e)}^{R(t_0)} R^{-\frac{1}{2}}\, dR = \frac{1}{\sqrt{\frac{\beta\, c^2\, \alpha}{3}}} \frac{R^{\frac{1}{2}}}{\frac{1}{2}} \Big|_{R(te)}^{R(t_0)}$$

$$= \sqrt{R}\, \frac{1}{\sqrt{\frac{\beta\, c^2 \alpha}{12}}} \Big|_{R(te)}^{R(t_0)} = \sqrt{R} \sqrt{\frac{12}{\beta\, c^2 \alpha}} \Big|_{R(te)}^{R(t_0)} = \frac{\sqrt{12\, R}}{\sqrt{\beta\, c^2 \alpha}} \Big|_{R(te)}^{R(t_0)}$$

$$r(t_e) —\ r(t_0) = \frac{\sqrt{12\, R(t_0)}}{\sqrt{\beta\, c^2 \alpha}} — \frac{\sqrt{12\, R(t_e)}}{\sqrt{\beta\, c^2 \alpha}} \tag{4.15}$$

Rewriting the modified redshift Equation (3.20) in the form

$$R(t_e) = \frac{R(t_0)}{1+f(z)} \tag{4.16}$$

and apply it in Equation (4.15) while setting $r(t_0)$= 0, gives

$$r(t_e) = \frac{\sqrt{12\, R(t_0)}}{\sqrt{\beta\, c^2 \alpha}} — \frac{\sqrt{12 R(t_0)}}{\sqrt{(\beta\, c^2 \alpha)\,(1+f(z))}} \tag{4.17}$$

4.2.2 Closed Universe

Setting $k = 1$, Equation (4.14) becomes

$$- \int_{r(t_e)}^{r(t_0)} \frac{1}{1+r^2} dr = \int_{R(t_e)}^{R(t_0)} \frac{dR}{\sqrt{R}\sqrt{\frac{\beta c^2 \alpha}{3} - 4R}} = \int_{R(t_e)}^{R(t_0)} \frac{dR}{\sqrt{R}\sqrt{\frac{\beta c^2 \alpha - 12\, R}{3}}} \tag{4.18}$$

Making use of the standard integral $\int \frac{1}{1+r^2}\,dr = \tan^{-1} r$ and setting $r(t_0) = 0$, this Equation can be integrated as shown:

$$\tan^{-1} r(t_e) = \int_{R(t_e)}^{R(t_0)} \frac{dR}{\sqrt{R}\sqrt{\frac{\beta c^2 \alpha}{3}\left(1 - \frac{12\,R}{\beta c^2 \alpha}\right)}}$$

$$\tan^{-1} r(t_e) = \int_{R(t_e)}^{R(t_0)} \frac{dR}{\sqrt{R}\sqrt{\frac{\beta c^2 \alpha}{3}}\sqrt{1 - \frac{12R}{\beta c^2 \alpha}}} \tag{4.19}$$

Let $\sin^2\theta = \frac{12R}{\beta\, c^2 \alpha} \;\Rightarrow R = \left(\frac{\beta c^2 \alpha}{12}\right)\sin^2\theta$

Such that

$$dR = \frac{\beta c^2 \alpha}{12}\, 2\sin\theta\cos\theta\; d\theta \quad \text{i.e.,}\; d(\sin^2\theta) = 2\sin\theta\cos\theta\; d\theta$$

and

$$\sqrt{R} = \sqrt{\frac{\beta c^2 \alpha}{12}}\,\sin\theta$$

also

$$\sqrt{1 - \frac{12\,R}{\beta c^2 \alpha}} = \sqrt{1 - \sin^2\theta} = \cos\theta \tag{4.20}$$

Substituting the above Equations into Equation (4.19) yields

$$\tan^{-1} r(t_e) = \int_{\theta(t_e)}^{\theta(t_0)} \frac{\frac{\beta\, c^2 \alpha}{12}\, 2\,\sin\theta\cos\theta\, d\theta}{\sqrt{\frac{\beta c^2 \alpha}{12}}\sin\theta\sqrt{\frac{\beta c^2 \alpha}{3}}\,\cos\theta} = \int_{\theta(t_e)}^{\theta(t_0)} \frac{\frac{\beta\, c^2 \alpha}{6}\,\sin\theta\cos\theta\, d\theta}{\frac{\beta c^2\,\alpha}{6}\sin\theta\,\cos\theta}$$

$$\tan^{-1} r(t_e) = \int_{\theta(t_e)}^{\theta(t_0)} d\theta = \theta\Big|_{\theta(te)}^{\theta(t_0)} \tag{4.21}$$

But from $\sin^2\theta$ above,

$$\theta = \sin^{-1}\sqrt{\frac{12\,R}{\beta c^2 \alpha}} \tag{4.22}$$

Thus,

$$\tan^{-1} r(t_e) = \theta\Big|_{\theta(te)}^{\theta(t_0)} = \sin^{-1}\sqrt{\frac{12R}{\beta c^2 \alpha}}\Big|_{R(te)}^{R(t_0)}$$

$$\tan^{-1} r(t_e) = \sin^{-1}\sqrt{\frac{12\,R(t_0)}{\beta c^2 \alpha}} - \sin^{-1}\sqrt{\frac{12\;R(t_e)}{\beta c^2 \alpha}} \tag{4.23}$$

Applying the modified redshift Equation (4.16) into Equation (4.23) yields

$$\tan^{-1} r(t_e) = \sin^{-1}\sqrt{\frac{12\,R(t_0)}{\beta c^2 \alpha}} - \sin^{-1}\sqrt{\frac{12\;R(t_0)}{(\beta c^2 \alpha)\,(1+f(z))}} \tag{4.24}$$

Taking the tangent on both sides of Equation (4.24), and use the standard identity

$\tan(A \pm B) = \frac{\tan A \;\pm\; \tan B}{1 \mp \tan A\ \tan B}$

It is obtained that

$$r(t_e) = \frac{\tan\sin^{-1}\sqrt{\frac{12\,R(t_0)}{\beta c^2 \alpha}} - \tan\sin^{-1}\sqrt{\frac{12\;R(t_0)}{(\beta c^2 \alpha)\,(1+f(z))}}}{1 + \tan\sin^{-1}\sqrt{\frac{12\,R(t_0)}{\beta c^2 \alpha}}\ \tan\sin^{-1}\sqrt{\frac{12\;R(t_0)}{(\beta c^2 \alpha)\,(1+f(z))}}} \tag{4.25}$$

Lets make use of the following standard identity on this Equation

$$\tan\theta = \frac{\sin\theta}{\cos\theta} = \frac{\sin\theta}{\sqrt{1 - \sin^2\theta}} \text{ and given that } \sin^2\theta = \frac{12\,R}{\beta c^2 \alpha}$$

Equation (4.25) can therefore be rewritten as

$$r(t_e) = \frac{\sqrt{\frac{12\,R(t_0)}{\beta c^2 \alpha}}\ \frac{1}{\sqrt{1 - \frac{12\,R(t_0)}{\beta c^2 \alpha}}} - \sqrt{\frac{12\;R(t_0)}{(\beta c^2 \alpha)\,(1+f(z))}}\ \frac{1}{\sqrt{1 - \frac{12\;R(t_0)}{(\beta c^2 \alpha)\,(1+f(z))}}}}{1 + \sqrt{\frac{12\,R(t_0)}{\beta c^2 \alpha}}\ \frac{1}{\sqrt{1 - \frac{12\,R(t_0)}{\beta c^2 \alpha}}}\ \sqrt{\frac{12\;R(t_0)}{(\beta c^2 \alpha)\,(1+f(z))}}\ \frac{1}{\sqrt{1 - \frac{12\;R(t_0)}{(\beta\, c^2 \alpha)\,(1+f(z))}}}}$$

which can be simplified as

$$r(t_e) = \frac{\sqrt{\frac{12\,R(t_0)}{\beta c^2\alpha - 12R(t_0)}} - \sqrt{\frac{12\,R(t_0)}{(\beta c^2\alpha)(1+f(z)) - 12\,R(t_0)}}}{1+12\,R(t_0)\frac{1}{\sqrt{(\beta c^2\alpha) - 12R(t_0)}}\frac{1}{\sqrt{(\beta c^2\alpha)(1+f(z)) - 12R(t_0)}}}$$

Which can further be writen in the form:

$$r(t_e) = \frac{\sqrt{12\,R(t_0)}\left\{\sqrt{(\beta c^2\alpha)(1+f(z)) - 12R(t_0)} - \sqrt{\beta c^2\alpha - 12\,R(t_0)}\right\}}{\sqrt{(\beta c^2\alpha) - 12\,R(t_0)}\,\sqrt{(\beta c^2\alpha)(1+f(z)) - 12R(t_0) + 12\,R(t_0)}} \tag{4.26}$$

4.2.3 Open Universe

Setting $k = -1$, Equation (4.14) becomes

$$-\int_{r(t_e)}^{r(t_0)} \frac{1}{1-r^2}dr = \int_{R(t_e)}^{R(t_0)} \frac{dR}{\sqrt{R}\sqrt{\frac{\beta c^2\alpha}{3} + 4R}} \tag{4.27}$$

This Equation can be integrated as shown:

$$\tanh^{-1} r \Big|_{r(te)}^{r(t_0)} = \int_{R(t_e)}^{R(t_0)} \frac{dR}{\sqrt{R}\sqrt{\frac{\beta c^2\alpha}{3}\left(1+\frac{12\,R}{\beta\,c^2\alpha}\right)}} \tag{4.28}$$

Setting $r(t_0) = 0$, gives

$$\tanh^{-1}(t_e) = \int_{R(t_e)}^{R(t_0)} \frac{dR}{\sqrt{R}\sqrt{\frac{\beta c^2\alpha}{3}\left(1+\frac{12\,R}{\beta c^2\alpha}\right)}} \tag{4.29}$$

Let $\sinh^2\theta = \frac{12\,R}{\beta c^2\alpha} \Rightarrow R = \left(\frac{\beta c^2\alpha}{12}\right)\sinh^2\theta$

Such that

$$dR = \frac{\beta c^2 \alpha}{12} 2\sinh\theta \cosh\theta \, d\theta \quad \text{i.e.,} \quad d(\sinh^2\theta) = 2\sinh\theta\cosh\theta\, d\theta$$

and

$$\sqrt{R} = \sqrt{\frac{\beta c^2 \alpha}{12}} \sinh\theta$$

also

$$\sqrt{1 + \frac{12\,R}{\beta c^2 \alpha}} = \sqrt{1 + \sinh^2\theta} = \sqrt{\cosh^2\theta} = \cosh\theta$$

Appropriate substitutions in Equation (4.29) using the above Equations give

$$\tanh^{-1}(t_e) = \int_{\theta(t_e)}^{\theta(t_0)} \frac{\frac{\beta c^2 \alpha}{12} 2\ \sinh\theta\cosh\theta\, d\theta}{\sqrt{\frac{\beta c^2 \alpha}{12}}\ \sinh\theta \sqrt{\frac{\beta c^2 \alpha}{3}}\ \cosh\theta} = \int_{\theta(t_e)}^{\theta(t_0)} \frac{\frac{\beta c^2 \alpha}{6}\ \sinh\theta\cosh\theta\, d\theta}{\frac{\beta c^2 \alpha}{6}\ \sinh\theta\ \cosh\theta}$$

$$= \tanh^{-1}(t_e) = \theta\Big|_{\theta(te)}^{\theta(t_0)} \tag{4.30}$$

But from $\sinh^2\theta$ above,

$$\theta = \sinh^{-1}\sqrt{\frac{12\ R}{\beta c^2 \alpha}} \tag{4.31}$$

Thus,

$$\tanh^{-1} r(t_e) = \theta\Big|_{\theta(te)}^{\theta(t_0)} = \sinh^{-1}\sqrt{\frac{12\,R}{\beta c^2 \alpha}}\ \Big|_{R(te)}^{R(t_0)}$$

$$= \sinh^{-1}\sqrt{\frac{12\,R(t_0)}{\beta c^2 \alpha}} — \sinh^{-1}\sqrt{\frac{12\,R(t_e)}{\beta c^2 \alpha}} \tag{4.32}$$

Applying the modified redshift Equation (4.16) into Equation (4.32) yields

$$\tanh^{-1} r(t_e) = \sinh^{-1}\sqrt{\frac{12\,R(t_0)}{\beta c^2 \alpha}} - \sinh^{-1}\sqrt{\frac{12\,R(t_0)}{(\beta c^2\alpha)\,(1+f(z))}} \tag{4.33}$$

Taking the tangent on both sides of Equation (4.33) and using the standard identity

$$\tanh\,(A \pm B) = \frac{\tanh A \pm \tanh B}{1 \mp \tanh A \tanh B}$$

gives

$$r(t_e) = \frac{\tanh\sinh^{-1}\sqrt{\frac{12\,R(t_0)}{\beta c^2\alpha}} - \tanh\sinh^{-1}\sqrt{\frac{12\,R(t_0)}{(\beta c^2\alpha)\,(1+f(z))}}}{1 + \tanh\sinh^{-1}\sqrt{\frac{12\,R(t_0)}{\beta c^2\,\alpha}}\,\tanh\sinh^{-1}\sqrt{\frac{12\,R(t_0)}{(\beta c^2\alpha)\,(1+f(z))}}} \tag{4.34}$$

Let us use the following identity on this Equation.

$$\tanh\theta = \frac{\sinh\theta}{\cosh\theta} = \frac{\sinh\theta}{\sqrt{1+\sinh^2\theta}} \text{ and given that } \sinh^2\theta = \frac{12\,R}{\beta c^2\alpha}$$

Equation (4.34) can be rewritten as

$$r(t_e) = \frac{\sqrt{\frac{12\,R(t_0)}{\beta c^2\alpha}}\;\frac{1}{\sqrt{\frac{\beta c^2\alpha + 12\,R(t_0)}{\beta c^2\alpha}}} - \sqrt{\frac{12\,R(t_0)}{(\beta c^2\alpha)\,(1+f(z))}}\;\frac{1}{\sqrt{\frac{(\beta c^2\alpha)(1+f(z)) + 12R(t_0)}{(\beta c^2\alpha)\,(1+f(z))}}}}{1 + \sqrt{\frac{12\,R(t_0)}{\beta c^2\alpha}}\;\frac{1}{\sqrt{\frac{(\beta c^2\alpha) + 12\,R(t_0)}{\beta c^2\alpha}}}\sqrt{\frac{12\,R(t_0)}{(\beta c^2\alpha)\,(1+f(z))}}\;\frac{1}{\sqrt{\frac{(\beta c^2\alpha)(1+f(z)) + 12R(t_0)}{(\beta c^2\alpha)\,(1+f(z))}}}}$$

which can be simplified as

$$r(t_e) = \frac{\sqrt{\frac{12\,R(t_0)}{\beta c^2\alpha - 12\,R(t_0)}} - \sqrt{\frac{12\,R(t_0)}{(\beta c^2\alpha)(1+f(z)) - 12R(t_0)}}}{1 + 12R(t_0)\,\frac{1}{\sqrt{(\beta c^2\alpha) - 12\,R(t_0)}}\,\frac{1}{\sqrt{(\beta c^2\alpha)(1+f(z)) - 12\,R(t_0)}}}$$

Which is further written in the form:

$$r(t_e) = \frac{\sqrt{12R(t_0)}\left\{\sqrt{(\beta c^2\alpha)(1+f(z)) + 12\,R(t_0)} - \sqrt{\beta c^2\alpha + 12\,R(t_0)}\right\}}{\sqrt{(\beta c^2\alpha) + 12R(t_0)}\,\sqrt{(\beta c^2\alpha)(1+f(z)) + 12R(t_0)} + 12\,R(t_0)} \tag{4.35}$$

The above three cases described by Equations (4.17), (4.26) and (4.35) can be written in one combined Equation that depends on one function of time, the scale factor $R(t)$ as

$$r(t_e)= \frac{\sqrt{12\,R(t_0)}\left\{\sqrt{(\beta c^2\alpha)(1+f(z))-12\,kR(t_0)}-\sqrt{\beta c^2\alpha-12\,k\,R(t_0)}\right\}}{\sqrt{(\beta c^2\alpha)-12k\,R(t_0)}\sqrt{(\beta c^2\alpha)(1+f(z))-12kR(t_0)}+12kR(t_0)} \qquad (4.36)$$

If it is defined

$$a^* = \beta c^2\alpha - 12kR(t_0) \qquad (4.37)$$

$$b^* = (\beta c^2\alpha)(1+f(z)) - 12kR(t_0) \qquad (4.38)$$

and considering that the cosmic time t_e depends on the evolution of the function $f(z)$, and therefore consider $r(t_e)$ as a function of $rf(z)$, such that Equation (4.36) can be written in new simplified form as

$$rf(z)= \frac{\sqrt{12\,R(t_0)}\,(\sqrt{b^*}-\sqrt{a^*})}{\sqrt{a^*b^*}+12k\,R(t_0)} \qquad (4.39)$$

To establish a function relation between light intensity, I from an emitting astronomical object on the modified redshift, $f(z)$, consider a star or galax emitting light at an absolute luminosity, L from a distant source positioned at the comoving radial coordinate $r = r_e$ at cosmic time t_e. Consider the light emitted by photons as they travel through the Universe towards the origin along the radial direction such that at time $t = t_0$, it is observed at the origin $r(t_0) = 0$) during a time interval dt_e. Suppose that at time $t = t_0$, $r(t_0) = 0$) an observer measures the brightness, I of that light which he receives at a redshift $f(z)$ and his location of reception of light is given by Equation (4.36). Equation (4.39) is time

reversal invariant. This light was emitted in the time interval $[t_e, t_e + dt_e]$, will pass the observer in the time interval $[t_0, t_0 + dt_0]$. During this process, there is photon number conservation as the radiation passes the Universe and the photons are redshifted relative to the emitted wavelength (increasing wavelength of their spectrum) leading to a decrease in their energy by a factor $\frac{1}{1+f(z)}$. Consequently, the energy that passes through the spherical Universe of radius $r = rf(z)$ during the interval $[t_0, t_0 + dt_0]$ is the same as the product of $\frac{1}{1+f(z)}$ and the energy emitted during the interval $[t_e, t_e + dt_e]$.

Expressing light intensity, I dependent on luminosity, L of luminous matter in the Universe as

$$I = \frac{L\, dt_e}{1 + f(z)\ S_r f(z))} \tag{4.40}$$

where S_r denotes the surface area of the sphere of radius, $r = rf(z)$ at time $t = t_0$.

Considering Equation (3.22) and apply the fact that light in the spherical Universe is moving in the negative all directions and use the coordinate radius range $r = 0$ to $r = rf(z)$ as

$$\int_{t_e}^{t_0} \frac{c}{R(t)} dt = \int_0^{rf(z)} \frac{1}{1+kr^2}\ dr \tag{4.41}$$

The negative sign comes due to the fact that light is moving in the negative all direction.

If light is emitted at time t_e, will reach the observer at a time t_0. In the same manner, light emitted at $t_e + dt_e$ will reach the same observer at $t_0 + dt_0$, and thus Equation (4.41) can be expressed as

$$\int_{t_e + dt_e}^{t_0 + dt_0} \frac{c}{R(t)} dt = \int_0^{rf(z)} \frac{1}{1+kr^2}\, dr \tag{4.42}$$

or

$$\frac{cdt_o}{R(t_o)} - \frac{cdt_e}{R(t_e)} + \int_{t_e}^{t_0} \frac{c}{R(t)} dt = \int_0^{rf(z)} \frac{1}{1+kr^2}\, dr \tag{4.43}$$

Substituting Equation (3.22) into Equation (4.43) gives

$$\frac{dt_e}{R(t_e)} = \frac{dt_0}{R(t_0)} \quad \Rightarrow$$

$$\frac{R(t_e)}{R(t_0)} = \frac{dt_e}{dt_0} \tag{4.44}$$

Which on using the modified redshift Equation (4.16) gives

$$\frac{R(t_e)}{R(t_0)} = \frac{dt_e}{dt_0} = \frac{1}{1+f(z)} \tag{4.45}$$

Given that the surface area of the sphere, $S_r f(z)$ as

$$S_r f(z) = \frac{4\,\pi r^2 f(z)\, R(t_0)^2}{[1+kr^2 f(z)]^2} \tag{4.46}$$

Substituting Equation (4.44) into Equation (4.40) and applying Equation (4.46) gives

$$I = \frac{L\left[1+kr^2 f(z)\right]^2}{(1+f(z))^2\, 4\,\pi r^2 f(z)\, R(t_0)^2} \tag{4.47}$$

Substituting Equation (4.39) into Equation (4.47) to obtain the solution

$$I(f(z) = \frac{L\left[\,1 + k\left(\frac{\sqrt{12\,R(t_0)}\,(\sqrt{b^*} - \sqrt{a^*})}{\sqrt{a^* b^*} + 12k(t)R(t_0)}\right)^2\,\right]^2}{\left(1 + f(z)\right)^2 4\pi \left(\frac{\sqrt{12\,R(t_0)}\,(\sqrt{b^*} - \sqrt{a^*})}{\sqrt{a^*\,b^*} + 12\,k\,R(t_0)}\right)^2 R(t_0)^2} \tag{4.48}$$

1.3 Number Density–Modified Redshift Relation

Suppose stars or galaxies under considerations are distributed uniformly in the Universe such that we can count the number of stars we observe in a given redshift. Number density is the number counts of distant astronomical objects enclosed in a given volume. Taking N as the number of stars per unit volume of space with metric given by

$$\frac{dr^2+r^2d\theta^2+r^2\sin^2\theta\,d\theta}{(1+kr^2)^2} \tag{4.49}$$

the volume element of the hyper–sphere surface is given as (Wamalwa, 2016)

$$\frac{r^2\sin\theta\,d\theta\,d\varphi\,dr}{(1+kr^2)^3} \tag{4.50}$$

Therefore the number of stars between r and dr is given as

$$\frac{4\pi r^2dr}{(1+kr^2)^3N} \tag{4.51}$$

Consider Equation (4.36) and rewrite it as a function of $f(z)$ as shown

$$r(f(z)=\frac{\sqrt{12\,R(t_0)}\left[\sqrt{(\beta c^2\alpha)(1+f(z)-12k\,R(t_0)}-\sqrt{\beta c^2\alpha-12k\,R(t_0)}\right]}{\sqrt{\beta c^2\alpha-12\,R(t_0)}\,\sqrt{(\beta c^2\alpha)(1+f(z))-12kR(t_0)}\,+12kR(t_0)} \tag{4.52}$$

Applications of expansion of powers of $f(z)$ in this Equation obtains that $rf(z)$ is proportional to $f(z)$ and Equation (4.52) reduces to

$$rf(z)=\sqrt{\frac{3\,R(t_0)}{(\beta c^2\alpha-12k\,R(t_0)}}\,f(z) \tag{4.53}$$

Differentiating Equation (4.52) with respect to $f(z)$ gives

$$\frac{dr}{df(z)} = r'f(z) = \frac{(\beta c^2 \alpha)^2 \sqrt{3\,R(t_0)}}{\sqrt{b^*}\left(\sqrt{a^* b^*} + 12\,k\,R(t_0)\right)^2} \tag{4.54}$$

with the application of

$a^* = (\beta c^2 \alpha)(1 + f(z)) - 12kR(t_0)\ ;\ b^* = (\beta c^2 \alpha)\big(1 + f(z)\big) - 12kR(t_0)$

Further we can assume the number galaxies to be enclosed within the coordinate hyper–sphere in the region of space $rf(z)$ and $rf(z) + df(z)$ as

$$nf(z)\,df(z) = 4\pi r^2 f(z)[1 + k\,r^2 f(z)]^3 N r'f(z) df(z) \tag{4.55}$$

Substituting Equations (4.39) and (4.54) into Equation (4.55) to obtain the solution

$$nf(z) = \frac{48\,\pi\,NR(t_0)\,(\beta c^2 \alpha)^2 \sqrt{3\,R(t_0)}\,(\sqrt{b^*} - \sqrt{a^*})^2}{\left[1 + k\left(\frac{\sqrt{b^*} - \sqrt{a^*}}{\sqrt{a^* b^*} + 12\,k\,R(t_0)}\right)^2\right]^3 \left[\sqrt{a^* b^*} + 12k\,R(t_0)\right]^4} \tag{4.56}$$

This Equation relates how the number density counts of galaxies evolves with with modified redshift $f(z)$. Combined with the light–intensity-redshift relation Equation (4.48) provides important analytical results research.

In the next section, theories that shift from the standard cosmological model and the contention that the redshift of luminous objects as a distance indicator at cosmological scales might be biased or inconsistent are studied reinforcing the idea of modifying the standard Friedmann model.

4.4 Test Models

In this section, one and two parameter modification of the standard redshift model is considered. These modified models of z based on the redshift–scale factor remapping concept have proved to be consistent with current astronomical data. In these models,

observational data has already been used in reconstructing parameter value constraints and slight perturbation of the parameter is implored. The overall goal is to underscore the robust theoretical underpinning of cosmic acceleration, irrespective of the ongoing debate surrounding the mysteries of dark matter and dark energy. The subtle variation in parameters serves the dual purpose of exploring additional statistically significant features of cosmic structures and revealing the resilience of the model under slight perturbations. The generic effects implied by the modified redshift is investigated in which the standard redshift is only a special function of $f(z)$ i.e., $z = f(z)$.

The equality:

$$z = z_0 \tag{4.57}$$

where z_0 is the observed redshift. This a standard assumption in all theoretical cosmological analyses and every mapping between the cosmic scale factor and the observed redshift is ascribed to gravity and the metric that determine the photon path propagation.

The first model considered is studied by (Bassett *et al*., 2015) in the form

$$f(z) = \alpha_1 z_0 + \alpha_2 (z_0)^2 \tag{4.58}$$

where, α_1 and α_2 are arbitrary parameters. Based on the observed Supernovae (SN) data, the modified redshift Equation (4.58) allows an Einstein de Sitter Universe to fit the observed Supernovae Hubble diagram as successfully as the standard Friedmann model.

Using Equation (4.57) in Equation (4.58), yields the first modified theoretical parametric model as

$$f(z) = \alpha_1 z + \alpha_2 z^2 \tag{4.59}$$

where α_1 and α_1 are arbitrary parameters.

The second model is proposed by (Wojtak & Prada, 2017). In this model, the ratio of the standard redshift model z to the observed redshift z_0 was idea motivated developing a non−parametric model of the form:

$$f(z) = z_0 + \gamma(z_0)^2 \tag{4.60}$$

where, $\gamma(z_0)$ is a free function z_0. The standard model and modified model agree when $\gamma(z_0) = 0$.

Applying Equation (4.57) in Equation (4.60) yields the second modified model as

$$f(z) = z + \gamma(z)^2 \tag{4.61}$$

where $\gamma(z)$ is a free function of z .

Another modified model is proposed based on modified redshift approach written as

$$f(z) = \frac{z}{\varepsilon} \tag{4.62}$$

where ε is a free parameter. This model is capable of allowing for both $z < \frac{z}{\varepsilon}$ and $z > \frac{z}{\varepsilon}$ besides recovering the standard redshift at $\varepsilon \to 1$, so that $\frac{z}{\varepsilon} \to z$. This is an essential feature as it ensures that the modified redshift does not affect the interpretation of cosmic microwave background observations (CMB). This model together with others above-mentioned offers an attractive method for observing buildup of cosmic structures and have

provided a powerful consistency test of the standard Friedmann model and have been used to investigate cosmic acceleration from a phenomenological or dark matter point of view. Therefore, the incorporation of these models into cosmological models presents a compelling and physically plausible avenue for advancing the understanding of the universe and offers a fresh perspective that may help resolve existing anomalies and contribute to a complete and more coherent cosmological framework.

The Tolman dimming light term $(1+z)^{-4}$ is another method that can modify the standard redshift relation. In a cosmologically expanding Universe, the effects of surface brightness of standard candles of luminous astronomical objects receding with redshift will dim by a term $(1+z\,)^{-4}$ in comparison to similar standard static candles; making standard candles at higher redshifts appear dimmer to the observer (Calvi *et al*., 2014). This dimming term affects all cosmological luminous objects and is consistent for all cosmological models regardless of the geometry applied provided the redshift luminosity relation is governed by the Friedmann model (Sandage, 2010). This make it difficult to detect progressively higher redshift galaxies due to effects caused by time dilation, redshifted light and geometry of the Universe as per the relation (Calvi *et al.*, 2014).

$$I_O = I_e\,(1+z)^{-4} \tag{4.63}$$

where I_O and I_e are the observed and intrinsic surface brightness of luminous astronomical objects respectively. The contribution of this term need to be accounted for in order to make correct predictions of matter distribution in the Universe. The dimming effect has contributed to our understanding of ionizing radiations produced by the galaxies and therefore cosmological models lacking correction of this term might not be accurate, since

the ionizing radiations produced by galaxies are proportional to the number of galaxies observed in the actual universe.

Light intensity evolution with redshift without dark energy is given as (Langa *et al*., 2017):

$$I = \frac{L\left[1 + k\left(\frac{\sqrt{12\,R(t_0)}\,(\sqrt{b^*} - \sqrt{a^*})}{\sqrt{a^*\,b^*} + 12\,k\,R(t_0)}\right)^2\right]^2}{(1+z)^2\,4\pi\left(\frac{\sqrt{12\,R(t_0)}\,(\sqrt{b^*} - \sqrt{a^*})}{\sqrt{a^*\,b^*} + 12\,k\,R(t_0)}\right)^2 R(t_0)^2} \qquad (4.64)$$

where a^* and b^* are as defined in Equations (4.37) and (4.38) respectively with $z \to f(z)$ in Equation (4.38).

Modifying the classical light intensity Equation (4.64) in view of Equation (4.63) gives a new formula for light intensity evolution of galaxies as

$$If(z) = \frac{L\left[1 + k\left(\frac{\sqrt{12\,R(t_0)}\,\sqrt{b^*} - \sqrt{a^*}}{\sqrt{a^*\,b^*} + 12k\,R(t_0)}\right)^2\right]^2}{(1+z)^6\,4\pi\left(\frac{\sqrt{12\,R(t_0)}\,\sqrt{b^*} - \sqrt{a^*}}{\sqrt{\sqrt{a^*\,b^*} + 12\,k\,R(t_0)}}\right)^2 R(t_0)^2} \qquad (4.65)$$

Equations (4.65) gives the modified redshift relativistic Friedmann Equation for describing dynamics and evolution of the Universe due to dimming of light. The question addressed is whether the standard redshift analytical solutions for an expanding Universe are consistent with additional hypothesis of dimming term and make comparison with modified models stated above.

In the next chapter, modified cosmological models studied above are investigated in the context of structure formation in the Universe.

CHAPTER FIVE
RESULTS AND DISCUSSION

5.1 Structure Formation in a Matter–Dominated Friedmann Universe

Structure formation and evolution of galaxies can be explained in terms of gravitation using the standard Friedmann model within the context of dark matter and dark energy scenarios (Lopez-Corredoira, 2017). However, the physical origin of dark energy appears to be a big challenging problem of current cosmology. Many authors have tried to explain cosmic acceleration by introducing a cosmological constant or dark energy dominated epoch. However, the physical origin of dark energy remains a mystery. Additionally, the cosmological constant problem, which includes a coincidence, and a fine–tuning problem is an important issue. The present values of the densities of dark energy and dark matter are of the same order of magnitude. Within the standard model, dark-energy density is constant and dark-matter density scales with the inverse third power of the cosmic scale factor this appears to be a coincidence since it requires extremely fine-tuned initial conditions in the early Universe. Both in the very early Universe and in the far future Universe these energy densities differ by many orders of magnitude (120 orders of magnitude separating dark energy from the Planck scale).

In case homogeneity, isotropy, or both are broken, the standard model cannot accurately predict the Universe evolution (Melia & Shevchuk, 2012).

This crossover period of the Universe from a matter–domination epoch to presently acceleration domination is one of the most important puzzle problem in cosmology referred to as late time transition (Aydiner *et al.*, 2022) It seems unlikely to proceed towards a comprehensive theory of cosmology without understanding this critical transition.

5.2 Graphical Results

This section embarks on the simulation of predictions derived from the analytical solutions of two cosmological models, namely the standard redshift Friedmann model and the modified redshift Friedmann model. The Equations governing light intensity and number density as functions of redshift are explicitly articulated for both models—Equations (4.48) and (4.56) for the modified Friedmann model. Through these simulations, the impact of cosmic accelerated expansion on galaxy formation is explained, distinguishing between the effects attributed to modified and unmodified redshift models. The overall goal is to underscore the robust theoretical underpinning of cosmic acceleration, irrespective of the ongoing debate surrounding the mysteries of dark matter and dark energy. As shall be seen later, the simulated results presented herein align consistently with other empirical findings thereby validating this approach.

The parameter values employed in these simulations are meticulously chosen, with constraints derived from cosmological observational data. Variations in parameters, achieved through a nuanced adjustment in the MATLAB application, shed light on the kind of universe expected from the model. For instance, parameters such as (α_1,α_2) = (1, 0) and (γ,α_2) = (1, 0) exhibit no discernible modification of the redshift, rendering both the standard and modified model in the absence of dark energy indistinguishable when MATLAB version R2017b simulations are run in the background. This is the special case when the modified model recovers the standard unmodified model. However, it is emphasized that only sufficiently small parameter values permit the formation of a universe conducive to hosting observers. Larger positive values induce rapid expansion, hindering the formation of gravitational structures, while large negative values precipitate a swift collapse, also precluding galaxy formation. The subtle variation in parameters

serves the dual purpose of exploring additional statistically significant features of cosmic structures and revealing the resilience of the model under slight perturbations. In addition, all of the models mentioned above show very little difference in the overall free parameter adjustment.

To experimentally obtain particular parametric values like α_1, α_2 once given observational data for the parametric function used and once a model has been chosen, as in our case (modified redshift relation for the Friedmann model), all that one needs to do is to fit the model onto the observational data to find the values of the model parameters (Bassett *et al*., 2015). This is usually conducted using various statistical methods depending on the nature of the data and researcher's objectives. A number of statistical tools may be used, e.g., maximum likelihood estimation (MLE) or Bayesian inference. The best-fit values of parameters provide a description of how the redshift scale factor evolves over time according to the chosen parametric model, and then one calculates the significance level to reject or accept the obtained values. Astronomical observables may include position (direction) of light emitted from, e.g., supernovae Type Ia or high-redshift quasars, the expansion rate of the universe, or flux among, others (Langa *et al*., 2017). Other parameters of interest may be obtained through normal relationships between physical quantities as the need arises.

For non-parametric models, the same procedure can be adapted to obtain, e.g., γ, except that one does not assume a specific function form for the relationship between variables. Instead, one aims to capture the data's underlying structure without imposing pre−defined shapes (Wojtak & Prada, 2017). One can then consider a suitable statistical technique such as finding a smooth curve or surface that best fits the data points in a way that minimizes

some measure of error or deviation. Finally, the confidence levels can be calculated for validating the results.

The choice between parametric and non—parametric approaches often depends on the underlying assumptions about the observational data and the desired flexibility in capturing the relationship between redshift and other variables (Tian, 2017); in our case, number density and redshift. Furthermore, in general, parametric and non-parametric values are not the same in cosmology, as they represent different approaches to modeling and analyzing cosmological data, except possibly where both types of values are used in conjunction to study different aspects of the universe.

Parameter values used in the modified redshift models are slightly varied for comparison under consistent matter density and curvature of the universe (Aydiner *et al*., 2022). All values employed in the codes adhere to existing statistical data.

To examine the initial effects of cosmic acceleration on galaxy formation in both models, graph the number density curves individually. Subsequently, it is observed that the more significant disparity in structure formation between the modified and unmodified Friedmann models makes it challenging to clearly discern the onset of the accelerated expansion of the universe (Wojtak & Prada, 2017). The standard redshift model exhibits a greater level of structure formation compared to the modified redshift model. Nonetheless, to evaluate the impact of introducing the modified model, both the standard redshift and modified redshift models without dark energy are graphed on the same scale for comparison.

The MATLAB codes employed in these simulations adhere to constants such as redshift running from z = 0 to z = 5, the density of the universe ranging from $\rho(t_0) = 3 \times 10^{-27}$ kgm^{-3} to $\rho(t_0) = 8.78 \times 10^{-25}$ kgm^{-3}, speed of light $c = 3 \times 10^8$ m/s, cosmic scale factor

$R(t_0) = 9 \times 10^{25}$ m (modifiable as needed), gravitational constant $G = 6.67 \times 10^{-11}$ m^3 kg^{-1} s^{-2}, and the geometric curvature of the universe, where $\kappa = 0$ signifies a Flat Universe, $\kappa = +1$ designates a Closed Universe, and $\kappa = -1$ represents an Open Universe (Langa *et al.*, 2017).

Figures 5.1—5.3 portray simulation outcomes for the evolution of light intensity for both the modified Friedmann model and the standard Friedmann model grounded in Equation (4.48). These visual representations offer a nuanced understanding of the intricate dynamics governing the evolution of cosmic structures under distinct cosmological paradigms. The standard redshift model displays the simulation results in solid lines while modified models are in dotted lines.

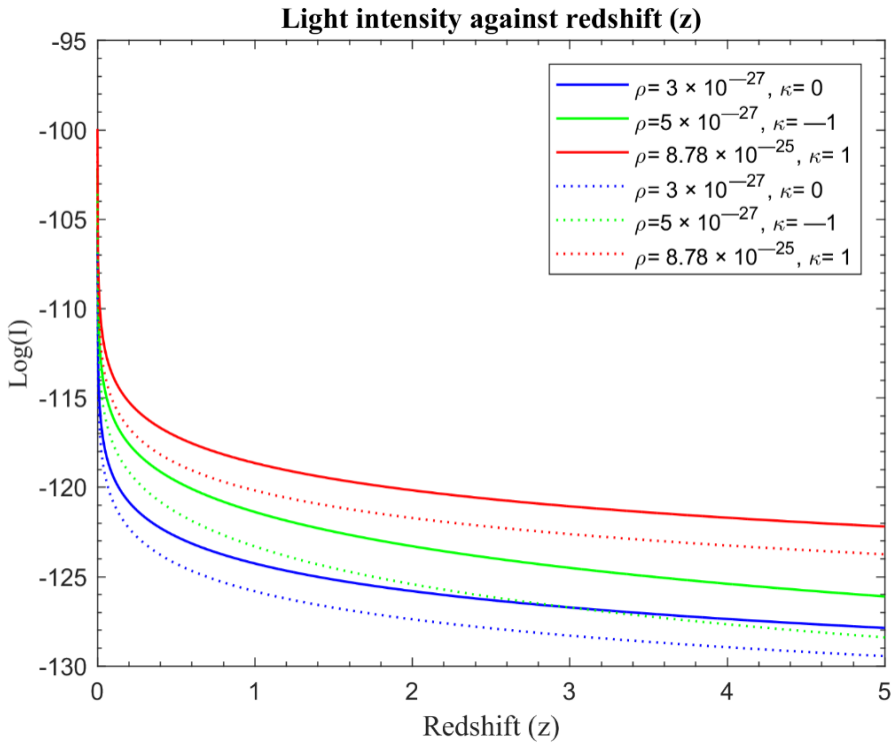

Figure 5.1 The modified redshift $f_1(z) = \alpha_1 z + \alpha_2 z^2$ with $\alpha_1 = 2.005$ and $\alpha_2 = 0.005$. The solid curves represent the standard redshift while dotted curves represent the modified redshift $f_1(z) = \alpha_1 z + \alpha_2 z^2$ with $\alpha_1 = 2.005$ and $\alpha_2 = 0.005$.

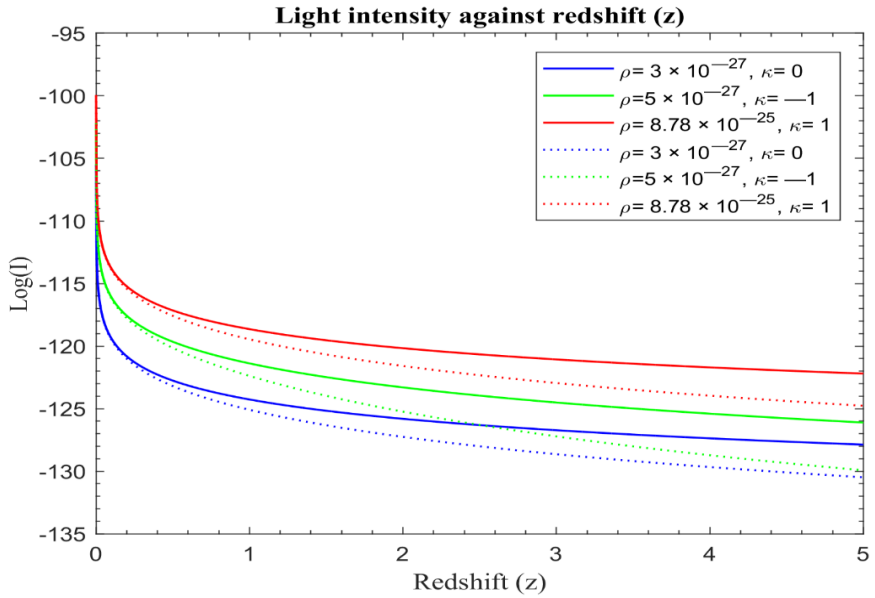

Figure 5.2 The modified redshift $f_2(z) = z + \gamma(z)^2$, where $\gamma(z)$ is a free function of z with $\gamma = 0.45$. The solid curves represent the standard redshift while dotted curves represent the modified redshift $f_2(z) = z + \gamma(z)^2$, where $\gamma(z)$ is a free function of z with $\gamma = 0.45$.

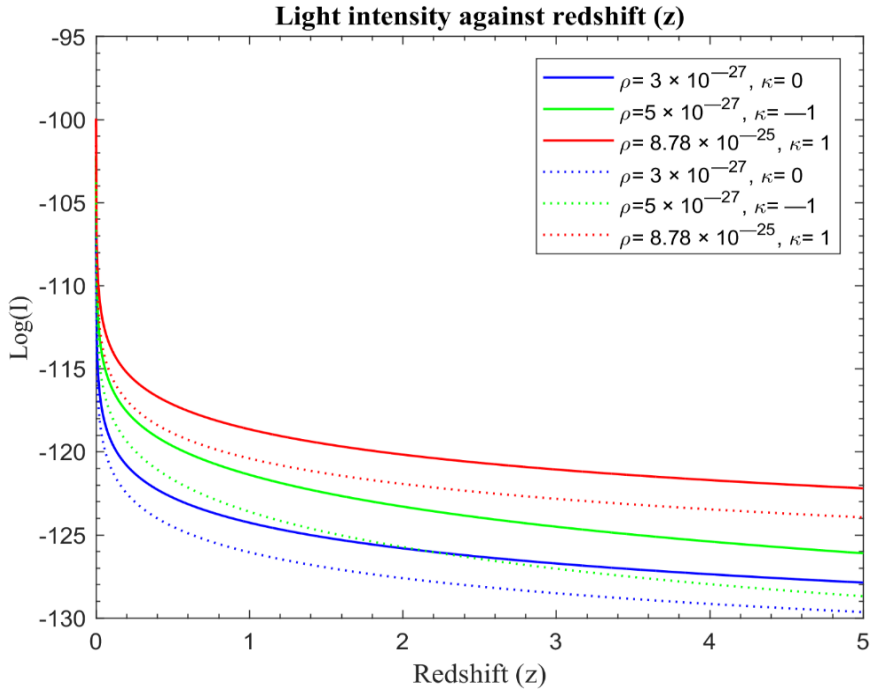

Figure 5.3 The modified redshift $f_3(z) = \frac{z}{\varepsilon}$ with $\varepsilon = 0.45$. The solid curves represent the standard redshift while dotted curves represent the modified redshift $f_3(z) = \frac{z}{\varepsilon}$ with $\varepsilon = 0.45$.

The number density of galaxies for the modified Friedmann model and the unmodified model are also graphed on the same scale in order to assess the overall effects. Figures 5.4–5.6 display the simulation results of number density of galaxy formation for the modified redshift Friedmann model based on Equation (4.56).

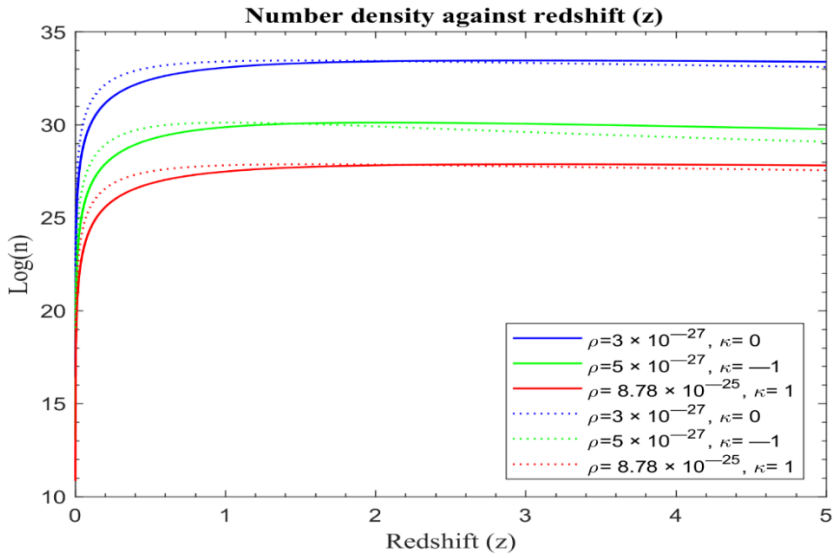

Figure 5.4 The modified redshift $f_4(z) = \alpha_1 z + \alpha_2 z^2$ with $\alpha_1 = 2.005$ and $\alpha_2 = 0.005$. The solid curves represent the standard redshift while dotted curves represent the modified redshift $f_4(z) = \alpha_1 z + \alpha_2 z^2$ with $\alpha_1 = 2.005$ and $\alpha_2 = 0.005$.

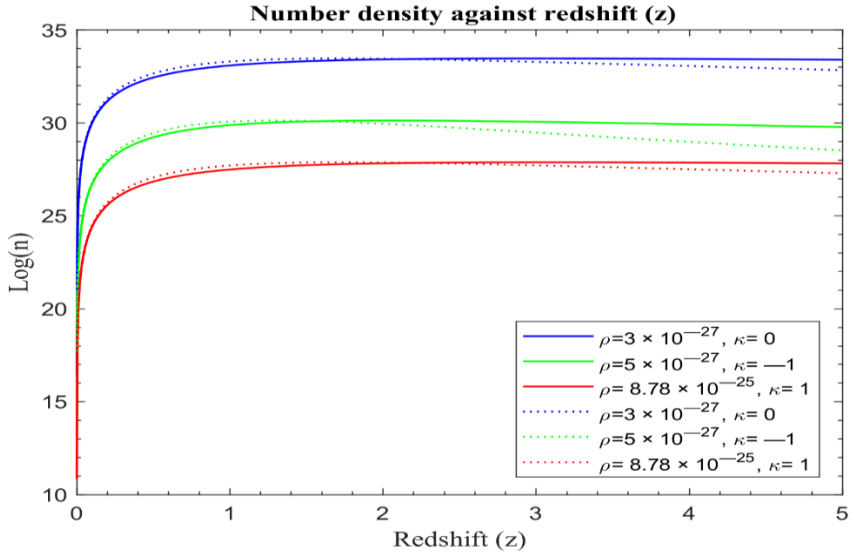

Figure 5.5 The modified redshift $f_5(z) = z + \gamma(z)^2$, where $\gamma(z)$ is a free function of z and $= 0.45$. The solid curves represent the standard redshift while dotted curves represent the modified redshift $f_5(z) = z + \gamma(z)^2$, where $\gamma(z)$ is a free function of z and $= 0.45$.

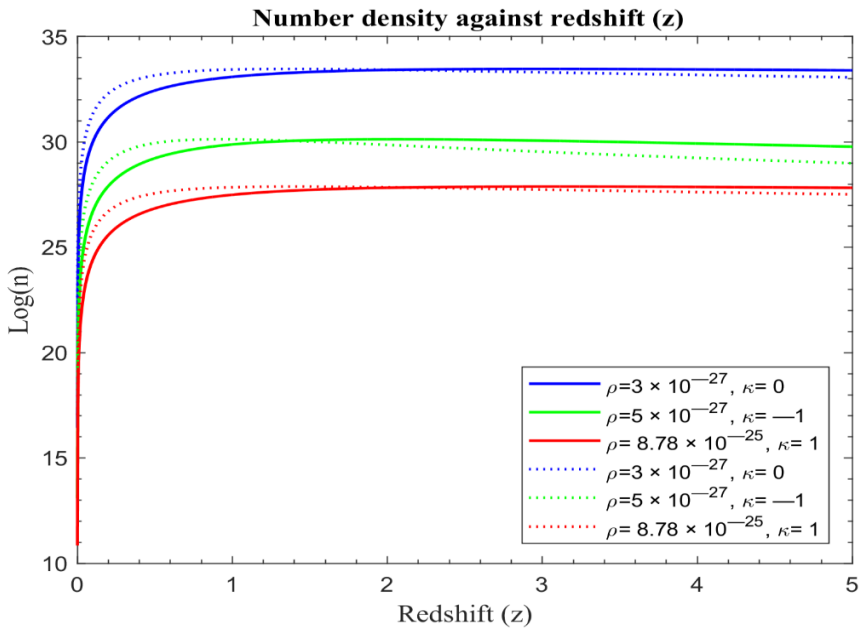

Figure 5.6 The modified redshift $f_6(z) = \frac{z}{\varepsilon}$ with $\varepsilon = 0.45$. The solid curves represent the standard redshift while dotted curves represent the modified redshift $f_6(z) = \frac{z}{\varepsilon}$ with $\varepsilon = 0.45$.

5.3 Discussion

5.3.1. Light Intensity of Galaxy Distribution

The attenuation of light intensity with redshift is visually depicted in Figures 5.1–5.3, covering various redshift ranges. In Figures 5.1–5.3, a distinct decrease in light intensity is evident across different universe models, transitioning from Flat to Open and then Closed Universes, regardless of the specific model applied. This attenuation is particularly pronounced in the modified redshift model, suggesting a potential phenomenological link between cosmic expansion and dark matter. Furthermore, the matter density and the curvature of the universe, as demonstrated by the similar attenuation rates between Open and Flat Universes within the redshift range of z ≈ 2–2.4 before diverging, influence this phenomenon.

Analyzing the range of redshifts depicted in Figures 5.1–5.3, a discernible exponential attenuation pattern in the light intensity from galaxies is observed, regardless of the

universe's geometry (Calvi *et al.*, 2014). Intriguingly, modified light curves closely resemble standard redshift curves, indicating a level of universality in light intensity dynamics. However, a notable deviation is evident in the evolution of these intensity functions, especially in the modified model, diverging from the standard redshift model in both early epochs, and in future projections. This temporal disparity aligns with theoretical propositions by (Langa *et al.*, 2017), who found that light intensity falls with redshift and is affected by dark energy, thereby bolstering the credibility of the modified model's departure from conventional cosmic models.

Results from (Grodzicka-Kobylka, *et al*., 2021) regarding light from GRBs also confirmed these findings. Moreover, the modified redshift Universe demonstrates a more rapid attenuation of light intensity with redshift compared to the standard redshift Universe, as depicted in Figures 5.1–5.3. This divergence underscores the accelerated expansion posited by the modified model, contributing to the ongoing debate on cosmological models. The empirical validation of this accelerated expansion, supported by theoretical foundations laid out by (Langa *et al.*, 2017), emphasizes the significance of investigating the intricate relationship between theoretical frameworks and observational data.

The attenuation behavior of light is in line with classical expectations (Lerner, 2018) . As redshift increases, the ionizing sources decrease because structure formation slows down (Langa *et al*., 2017).. Furthermore, space expansion and redshifted photons leads to energy loss. Furthermore, an analysis of light pulse shapes originating from gamma rays, slow and fast neutron events, recorded separately using the Bollinger–Thomas single-photon method, showed a trend consistent with our results (Grodzicka-Kobylka, *et al*., 2021).

This advantage also exists with models due to dimming light (Calvi *et al*., 2014). A graph of light intensity with redshift based on Equation (4.65) is as shown below.

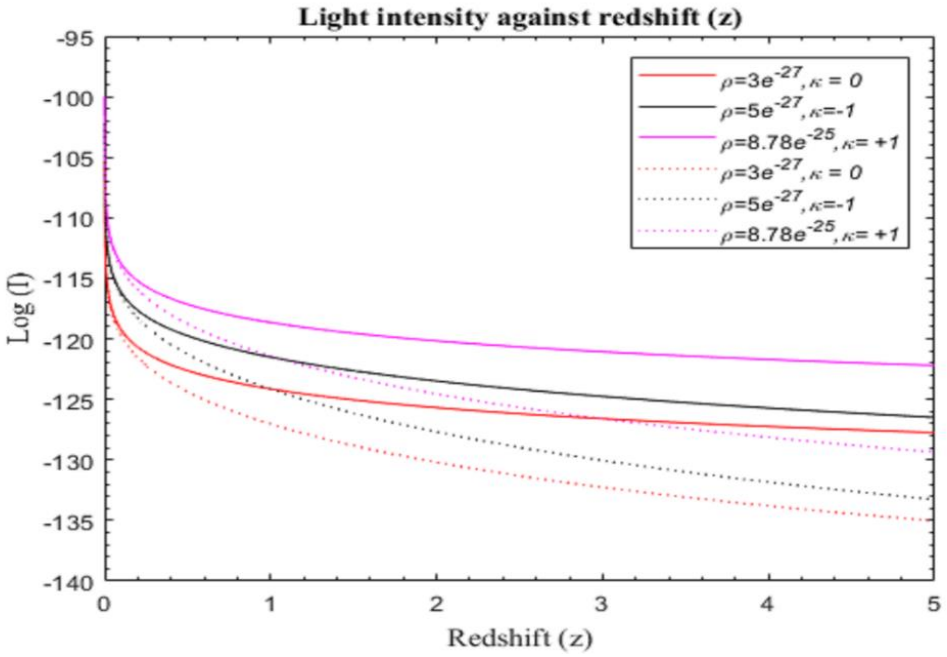

Figure 5.7 The modified redshift $f_7(z) = z$ with Tolman's correction term. The solid curves represent log (I) against standard redshift z while the dotted curves represent log (I) against modified redshift *z* with Tolman's correction term for z = 0 to z = 5 .

Figure 5.7 shows that for both Tolman's redshift model and standard redshift model, the light intensity decreases rapidly with redshift for z = 0 to z = 5 in agreement with earlier findings (Lerner, 2018) validating them.

5.3.2. Number Density of Galaxy Formation

The data represented in Figures 5.4–5.6 reveal intriguing patterns wherein the modified redshift curves initially display accelerated growth, contrasting with the standard redshift model. However, both curves stabilize for a duration before diverging. Beyond a redshift value of z ≈ 1.6, the modified redshift curves start descending below those of the standard redshift. There is a phase of heightened galaxy formation within the redshift range of 0 <

$z < 0.4$ across all universe models. Additionally, a significant proportion of galaxy formation appears to have occurred during $0 < z < 0.9$, persisting, albeit at a slower pace, until around $z \approx 1.6$. This observation is consistent with Marr's findings (Marr, 2023), who studied galaxy number counts in various bands (K, H, I, R, B, U) from the Durham Extragalactic Astronomy and Cosmology catalogue. In the model, bar graphs revealed a similar relationship between number density and redshift. Studies of initial formation and evolution of spiral galaxies dataset in the CANDELS fields for the number density of galaxies against redshift in the range $1 < z < 3$ further confirms our findings (Bentabol, *et al*., 2022).

Around $z \approx 0.9$, the rate of galaxy formation in the modified redshift model decreases, unlike the relatively steady formation rate in the standard redshift model. This discrepancy suggests that the modified redshift model, indicative of a universe propelled by dark matter dynamics, fosters galaxy formation especially in the beginning. This finding agrees with (Junwe *et al.*, 2023), who investigated the impact of dark matter on galaxy formation using N-body simulations. He found that baryonic matter gravitates towards great potential wells of dark matter halos where galaxies form initially rapidly before slowing down later. However, the rate of formation is intricately tied to both the matter density of the universe and its curvature characteristics.

In examining the early stages of the universe, characterized by the initial burst of galaxy or star formation, a remarkable uniformity is observed among our models. The accelerating expansion of space, a key determinant in rendering any future accretion negligible, serves as a unifying factor at this emerging cosmic era (Bentabol *et al*., 2022).

The indistinguishability of each model at early times lays the foundation for understanding the subsequent divergences in their evolutionary trajectories (Bassett *et al*., 2015).

The historical divergence among these models becomes conspicuous in the late stages, primarily attributable to the onset of dark-matter─powered accelerated expansion (Junwe *et al*., 2023). A notable consequence of this divergence is the elimination of the coincidence problem. Scenarios where λ equals zero equates to the era of matter growth that propels the cosmic accelerating force responsible for the late─time spatial acceleration (Tian, 2017). In the modified case, the departure from the standard redshift Friedmann model continues throughout all cosmic epochs, marking a significant achievement in this research.

The number density of galaxy formation exhibits a rapid rise, culminating around $z \approx 1.6$, followed by a gradual decline. The proposed model seems to undergo a phase of deceleration favoring galaxy formation in the early evolution of the universe, transitioning into an acceleration phase late times. This critical transition from early deceleration to late─time acceleration is pivotal, as the decelerating phase is important for structure formation, while the slowdown of large-scale structure growth signifies the onset of dominant accelerating cosmic expansion (Aydiner *et al*., 2022). This observation is in line with recent work that suggests that dark matter provides the initial seed for star formation (Milakovic *et al*., 2023) further boost these findings.

As galaxies disperse due to the expanding universe, the processes of accretion and merging decelerate significantly, leading to a substantial reduction in the galaxy formation rate after peaking for future epochs (Riess *et al*., 1998). The total number density is predominantly dictated by contributions from the peak, stabilizing into a plateau around $z \approx 1.6$ depending on the curvature characteristics and matter density. Figures 5.4–5.6

underscore that the universe, largely, has already produced the majority of its eventual structures, contributing only marginally to future developments.

The number density of galaxies increases with redshift with a remarkably constant value after peaking for the standard model for future epochs, while that of the modified model declines slowly thereafter peaking. The drop in galaxy number may be attributed to a fast increase in light intensity attenuation; producing strong repulsive forces at high redshifts (see light intensity curves in Figures 5.1–5.6). For future epochs, gravitational forces may play a role in controlling the rate of decline, with the repulsive forces originating in light attenuation being negligible.

5.3.3. Transition from Decelerating to Accelerating Expanding Universe

This section concentrates on identifying the suppression point within the structure amplitude, a key aspect of our simulation concerning the number density of galaxies. This investigation aids in predicting the transition point between deceleration and acceleration in our modified cosmological model.

A comprehensive analysis of Figures 5.4–5.6 reveals a significant trend in galaxy formation. In the early stages of the universe, galaxies form rapidly, experiencing a burst of stellar or galactic activity between redshift $0 < z < 0.4$. This rate peaks around $z \approx 0.9$ before slowing down significantly, maintaining a relatively constant level of galaxy formation until $z \approx 1.6$ where this process starts to decline, as evident in Figures 5.4–5.6. This result agrees with (Bentabol *et al*., 2022), who found that the onset of cosmic acceleration was consistent with observations of distant spiral galaxies exhibiting a gradual decline or near constancy in galaxy formation over time.

The universe may have undergone a shift from a phase of decelerating expansion after its climax to accelerated expansion. The universe undergoes a series of redshift transitions, as demonstrated by (Riess *et al*., 1998), who noted the universe's mass-energy content transitions from matter domination to an acceleration-dominated state. The persistence of accelerated expansion requires overcoming gravitational attraction forces exerted by the cosmological fluid, primarily composed of ordinary matter.

In this model framework, the transition from deceleration to acceleration expansion occurs at a specific redshift. These findings suggest that a transition from matter domination to acceleration expansion is feasible only if the energy effects driving the universe into acceleration begin in an epoch $z \approx 0.9$. This value is in fair agreement with the best─fit value of $0.732 < z < 0.966$ (Kumar *et al*., 2023). However, any observed disparities with other models could stem from variations in models or underlying assumptions used. However, pinpointing the accurate redshift transition point requires calibrating model parameters against cosmological data. (Aydiner *et al*., 2022) predicts a plausible temporal transition from a matter─dominated universe to a dark─energy-dominated universe, emphasizing the importance of fitting model parameters to observational data for precise and reliable cosmological predictions.

5.3.4. Comparing the Modified Redshift Friedmann Cosmological Models

Within this section, the primary focus is on comparing the inherent properties of three modified cosmological models: the modified redshift Friedmann models. The simulation of the three modified models are on the same scale in order to assess the implications of the modified models on luminous matter distribution in the modified Friedmann Universe.

Figure 5.8 shows the simulation of light intensity of the three modified models.

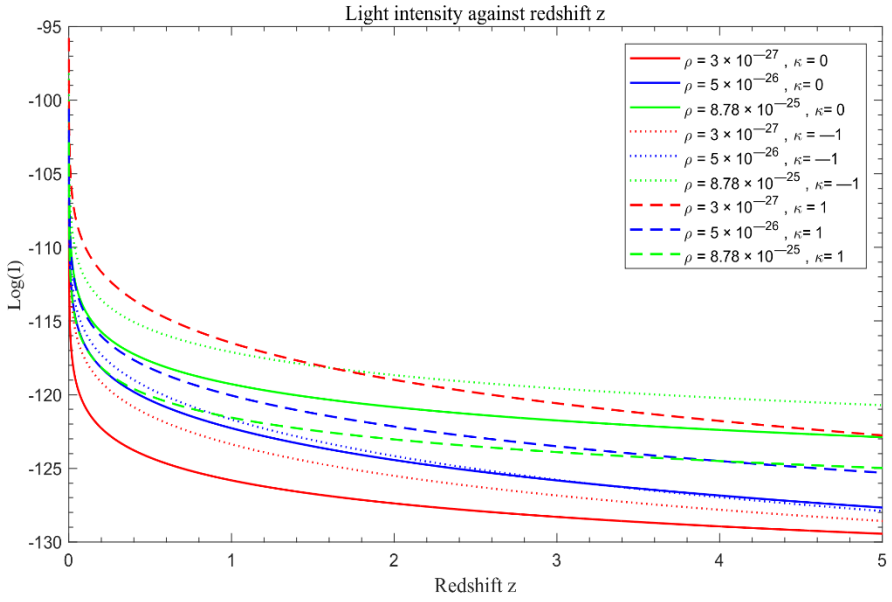

Figure 5.8 Log (I) against the modified redshift $f_8(z)$. The solid curves represent the modified redshift $f_1(z) = \alpha_1 z + \alpha_2 z^2$, the dotted curves represent the modified redshift $f_2(z) = z + \gamma(z)^2$ while the dotted curves represent the modified redshift $f_3(z) = \frac{z}{\varepsilon}$. The parameter constraints remains as earlier defined.

The solid curves portray the simulated result of light intensity modified redshift models: $f_1(z) = \alpha_1 z + \alpha_2 z^2$, $f_2(z) = z + \gamma(z)^2$ and $f_3(z) = \frac{z}{\varepsilon}$ illustrated by the red, blue and green colours respectively for the different curvature scalars based on Equation (4.48). The dotted curves represent Open Universes while the dashed curves represent Closed Universes.

The observed attenuation behavior of light is in line with classical expectations with the disparity arising from the variation of the Universe geometry.

The number density of galaxies with modified redshift of the three modified models adopted are also on the same scale based on Equation (4.56). The solid curves Figure 5.9 portray the simulated result of number density of galaxies of the modified redshift models

adopted above $f(z) = \alpha_1 z + \alpha_2 z^2$, $f(z) = z + \gamma(z)^2$ and $f(z) = \frac{z}{\varepsilon}$ represented by red, blue and green colours respectively for the different geometry of the universe and are all based on Equation (4.56). The dotted curves represent Open Universes while the dashed curves represent Closed Universes.

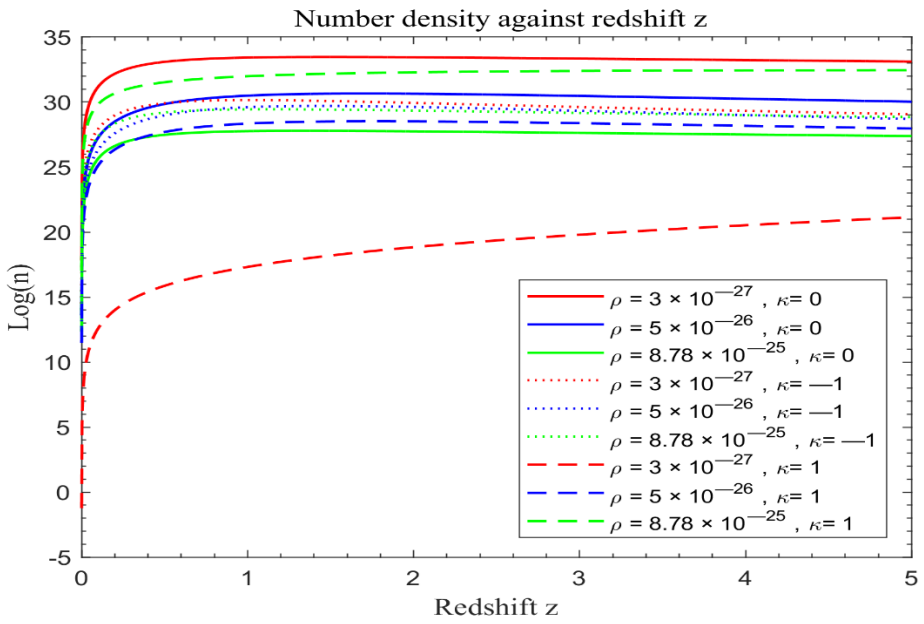

Figure 5.9 Log (n) against the modified redshift $f_9(z)$. The solid curves represent the modified redshift $f_1(z) = \alpha_1 z + \alpha_2 z^2$, the dotted curves represent the modified redshift $f_2(z) = z + \gamma(z)^2$ while the dotted curves represent the modified redshift $f_3(z) = \frac{z}{\varepsilon}$. The parameter constraints remains as earlier defined.

While different simulations of the modified Friedmann model show varied galaxy formations, both models demonstrate a consistent overall galaxy formation history (see Figure 5.9). Graphical representations illustrate a notable disparity between the trajectories outlined by the three modified redshift models. This clear distinction serves as empirical evidence of the influence of dark matter driving accelerated expansion. Despite this gap, both cosmologies share a commonality in the culmination of galaxy formation in the early universe. Briefly, while both models statistically aligns with each other, a distinctive trajectory emerges at all stages of the universe due to the influence of the

geometry of the Universe. Structure formation is more in a Flat Universe followed by Open and then Closed Universes. Despite subtle variations in underlying mechanisms, these models converge on the same analytical outcome concerning the magnitude of observed structure formation. Indeed, Figures 5.9 illustrate trajectories of different structures formed by modified redshift models, indicating a notable disparity and suggesting the pivotal role of geometry of the Universe and dark matter in late-time acceleration. These findings underscore the complexity of cosmic dynamics and highlight the intricate interplay between various factors influencing the evolution of our expansive Universe.

CHAPTER SIX
CONCLUSIONS AND RECOMMENDATIONS

6.1 Summary Conclusions

The present astronomical inquiry stands as a diligent effort to scrutinize the fundamental principle of cosmology, specifically addressing the homogeneity and isotropy assumptions inherent in the Friedmann model. Extensive research has dedicated to testing spatial isotropy through a spectrum of techniques and probes. Nevertheless, the homogeneity hypothesis presents a formidable challenge, prompting a focused investigation (Kim *et al*., 2022). This study focused on three fundamental astronomical quantities: number density, light intensity, and redshift. It explores the interrelationship between these quantities in both the standard redshift Friedmann model and its modified form proposed within the research. The study extends the groundwork laid by prior research on the Friedmann model (Langa *et al*., 2017). The driving force arises from a modification of the conventional redshift, providing a fresh perspective on the Friedmann Equations. This reinterpretation grounded in a phenomenologically modified redshift model, deliberately devoid of dark energy through the elimination of the cosmological constant.

The modified redshift, as introduced in this study, serves as a novel instrument for characterizing the distribution of luminous matter within the cosmic framework validating the Friedmann model particularly in investigation the growth of large-scale cosmic structures.

This parameter emerges as a discerning factor, keen to differentiate between the General─Relativity-backed standard redshift Friedmann model and the alternative

scenarios rooted in its modified form. The overall goal is to establish a framework for discerning between competing cosmological models.

Distinct phenomenologically modified redshift models, namely parametric and non—parametric models systematically explored within the context of a matter—dominated Friedmann Universe. The analytical prowess of this study demonstrated through the rigorous solution of relativistic dynamic Friedmann Equations as given in Equations (4.48), (4.56) and (4.65). Compared to earlier research (Langa et al., 2017), Equations (4.48), (4.56), and (4.65) are more generalized form, describing the relationship between light intensity and redshift, as well as the relationship between number density and redshift. These solutions, in turn, shed light on the light intensity and number density of galaxies, describing their evolution as functions of the modified redshift as seen in Figures 5.1–5.3 and Figures 5.4–5.6, respectively.

Simulations meticulously executed utilizing MATLAB applications. The simulation spans the redshift range from 0 to 5, revealing intriguing dynamics. The simulation reveals a unique pattern of galaxy formation, marked by a significant burst between redshifts $0 < z < 0.4$. This burst then transitions into a gradual rise up to $z \approx 0.9$, after which galaxy formation proceeds slowly at a nearly constant rate until $z \approx 1.6$. Thereafter, a decline in structure formation becomes possible, as illustrated in Figures 5.4–5.6. Furthermore, simulations without dark energy unveil a phase crossover point in the cosmic galaxy formation rate, marking the transition from deceleration to accelerating expansion at redshifts around $z \approx 1.6$, as seen from Figures 5.4–5.6. Our number density relation is in excellent agreement with other works (Bentabol, *et al*., 2022).

Simulations of light intensity functions reveal light attenuation with redshift evident in Figures 5.1–5.3, which is in fair agreement with the GRB results and light pulse distribution shapes (Grodzicka-Kobylka, *et al*., 2021). The modified redshift universe shows that light intensity distribution attenuates more rapidly with the standard redshift as compared to the modified redshift model (Figures 5.4–5.3).

A critical observation emerges concerning the differential impact of the standard model on structure formation. The study posits that the standard model exhibits a less pronounced effect on late—time structure growth compared to the modified model in agreement with observational evidence. This nuanced disparity underscores the prowess of the modified model. This work attributes the expansion of the universe beyond $z > 0.9$ to dark matter—powered cosmic acceleration (Figures 5.4–5.3). Despite differences in the rate of structural growth, the impact of accelerated expansion becomes only significant after majority of structure formation.

The thesis concludes with a resolute stance against the necessity of introducing the cosmological constant in the standard cosmological scenarios. The modified Friedmann model adopted here has characteristics of a positive cosmological constant in the context of the standard redshift model eliminating the need for a cosmological constant, and eliminating the necessity for fine-tuning at an implausibly small degree. The relentless acceleration of the universe in its later stages is firmly established and almost model-independent theoretical certainty, unaffected by ongoing debates about the nature of the cosmological constant.

The proposed modified model's ability to capture most of the discernible signatures of cosmic acceleration accurately underscores its novelty. Therefore, the expansion evolution of the universe might be a result of the imbalance of gravitational forces and dark matter.

The call for future inquiry echoes a commitment to testing with future accurate cosmological data. This paper, rooted in the analysis and scrutiny of cosmological models, contributes to the ongoing debate on the dynamic evolution of our universe.

6.2 Recommendations for Further Work

The modified redshift cosmological model adopted here has the potential to solve physical cosmology problems such as singularity, cosmic coincidence, time evolution of the Universe, future and fate of the Universe. Therefore, the modified redshift model deserve more attention for further studies since it is more general to many linear or non-linear interacting components. With this motivation, it is believed that the method presented in this study provides a good mathematical tool to study the apparent late time acceleration expansion of the Universe by obtaining a metric-dependent solutions and discuss the open problems mentioned above. The proposed modified model's ability to capture most of the discernible signatures of cosmic acceleration accurately underscoring its novelty. The call for future inquiry echoes a commitment to testing with future accurate cosmological data. In particular determine whether or not there was a singularity in the early Universe after the end of inflating period. There are hints of an existing singularity in the plots above; the light intensity curves Figures 5.1—5.3 take infinite values for light intensity around $z \approx 0$.

In order to get a better picture about early and future time dynamics of the Universe, the modified model should be extended to the multiple scalar parameters reconstructed from observational data. Additionary, some open problems in the present cosmology such as the observed values of vacuum energy density and the theoretical large values of zero

point energy obtained by Quantum Field Theory need further study. Careful scrutiny of the key assumption of supernova cosmology may also stem other potential problems.

Based on the current observational data, it is quite clear that the modified model just like the standard model exhibit the same characteristic behavior of light intensity and number density of galaxy formation and evolution with redshift. This consistency test is a confirmation of the validity of the standard Friedmann model. However, there still doubts on the quantity of data available and the present technology. Future galaxy survey experiments such as the recent detections of gravitational waves by the LIGO-Virgo collaborations; with improved sensitivity configurations together with the advent of the forth-coming detectors such as Einstein Telescopes will provide enormous data in many astronomical fields and are expected to improve the quality of data for a final say on this matter revealing cosmic explosions and effects of dark matter (Brough, *et al*., 2020).

REFERENCES

Alpher, V. (2014). The Prediction of the Cosmic Microwave Background Radiation. *Asian Journal of Physics*, 17-26.

Amendola, L., (1998). Homogeneity and Flactality. *The Astrophysical Journal*, 1-80.

Amendola, L., & Palladino, E. (1999). The Scale of Homogeneity in the Las Campanas Redshift Survey. *The Astrophysical Journal*, L1-L4.

Aydiner, E., Basaran-Öz, I., Dereli, T., & Sarisaman, M. (2022). Late time transition of the universe and the hybrid scale factor. *The European Physical Journal C*, 82-39.

Bassett, B., Fantaye, Y., Hlozek, R., Sabiu, C., & Smith, M. (2015). A Tale of Two Redshift. *arXiv:1312.2593v1[astro-ph. Co]*, 1-9.

Bentabol, B., Conselice, C., Haeussler, B., Csteels, K., Lintott, C., Masters, K., & Simmons, B. (2022). Observations of the initial formation and evolution of spiral galaxies at $1 < z < 3$ in the CANDELS fields. *Mon. Not. R. Astron. Soc.*, 1502–1517.

Bolejko, K., Celerieri, M., & Krasinski, A. (2011). Inhomogeneous Cosmological Models: Exact solutions and their applications. Classical and Quantum Gravity. *arXiv: 1102. 1449 [astro-ph. CO]*, 1-32.

Brough, S., Collins, C., Demarco, R., Henry, C., Ferguson, Galaz, G., Montes, M. (2020). The Vera Rubin Observatory Legacy Survey of Space and Time and the Low Surface Brightness Universe. *Proceedings IAU Symposium*, 1-7.

Calvi, V., Stiavelli, M., Bradley, L., Pizzella, A., & Kim, S. (2014). The Effect of Surface Brightness dimming in the selection of High Z Galaxies. *The Astrophysical Journal*, 102-796.

Clowes, R., Harris, K., Raghunathan, S., Campusano, L., Sochting, I., & Graham, M. (2013). A structure in the early Universe at z= 1.3 that exceeds the homogeneity scale of the R-W concordance cosmology. *Monthly Notices of the Royal Astronomical Society*, 2910-2916.

Conn, A., Lewis, G. F., Ibata, R. A., Parker, Q., Zucker, D. B., McConnachie, A. W., Chapman, S. (2013). The Three Dimensional Structure of the M31 Satellite System; Strong Evidence for an Inhomogeneous Distribution of Satellites. *The Astrophysical Journal*, 1-16.

Durrer, R., & Labini, F. (1998). A Fractal Galaxy Distribution in a Homogeneous Universe? *Astron.Astrophys.* , L85-L88.

Einstein, .A, (1915). The Field Equations of Gravitation. *Proceedings of The Prussian Academy of Sciences*, 844-847.

Einstein, .A, (1917). Cosmological Considerations in the General Theory of Relativity. *Konigl. akademie der wissenschaften*, 142-152.

Einstein, .A, (1931). Zum kosmologichen Problem der allgemeinen Relativitatstheorie. *Sitzungsber. Preuss. Akad. Wiss. Berlin (Math. Phys)*, 235-237.

Ellis, G. (2011). Inhomogeneity effects in Cosmology. *Class.Quant.Grav. 28 (2011) 164001*, 1-29.

Friedmann, A. (1922). On the curvature of space. *Zeitschrift Fur Physik*, 377-386.

Gomez, S. (2011). On Friedmann-Lemaitre-Robertson-Walker cosmologies in non-standard gravity. *ArXiv: 1104. 0813v1*, 193.

Grijs, R. (2012). Advancing the Physics of Cosmic Distances: Conference Summary. *IAU Symp. 289*, 351.

Grodzicka-Kobylka, M., Szczesniak, T., Swiderski, L., Brylew, K., Moszynski, M., Valiente-Dobon, J., Mianowska, Z. (2021). Comparison of detectors with pulse shape discrimination capability for simultaneous detection of gamma-rays, slow and fast neutrons. *Nucl. Instrum. Methods Phys. Res.*, 165858.

Hubble, E. (1926). Extragalactic nebulae. *Astrophysical Journal*, 321-369.

Humay, M., Philips, M., Aviles, R., & Maza, J. (1995). A Hubble Diagram of Distant Type IA Supernovae. *The Astronomical Journal*, 109.

Joyce, M., Labini, F., Gabrielli, A., Montuori, M., & Pietronero, L. (2005). Basic properties of galaxy clustering in the light of recent results from the Sloan Digital Sky Survey. *arXiv:astro-ph/0501583v2*, 11-16.

Junwe, D., Shibiao, W., Zherui, W., & Chang, L. (2023). The impact of the dark matter on galaxy formation. *J. Phys. Conf. Ser.*, 2441.

Kim, Y., Park, C., Noh, H., & Hwang, J. (2022). CMASS galaxy sample and the ontological status of the cosmological principle. *Astron. Astrophys.*, A139.

Kumar, D., Jain, D., Mahajan, S., Mukherjee, A., & Rana, A. (2023). Constraints on the transition redshift using Hubble phase space portrait. *Int. J. Mod. Phys.*, 2350039.

Kuzmichev, V., & Kuzmichev, V. V. (2024). The Hubble tension from the standpoint of quantum cosmology. *Eur. Phys. J. C*, 84-121.

Labini, F. (2011). Inhomogeneities in the universe. *Class.Quant.Grav.*, 1-30.

Labini, F., Montuori, M., & Pietronero, L. (1998). Scale-invariance of galaxy clustering. *Phys.Rept.*, 61-226.

Lahav, O. (2017). 100 years of the Cosmological Constant: What's next? *arXiv prep. arXiv:1704.00069 [Astro-Ph]*, 1-13.

Langa, M., Wamalwa, D., & Mito, C. (2017). Relativistic Dynamics in a matter-Dominated Friedmann Universes. *Journal of Astrophysics and Astronomy*, 38-71.

Lemaitre, G. (1927). Republican of: A homogeneous Universe of Constant Mass and Growing Radius Accounting for the Radial velocity of Extragalactic Nebulae. *Annales Soc. Sci. Bruxelles, Pubbl. Lab. Astron. Geodesie. An English Translation by, Gen. Rel. Grav*, 188-192.

Lerner, E. (2018). Observations contradict galaxy size and surface brightness predictions. *MNRAS*, 3185–3196.

Lopez-Corredoira, M. (2017). Tests and problems of the standard model in cosmology. *Found.Phys.*, 711-768.

Marr, J. (2023). Faint Galaxy Number Counts in the Durhamand SDSS Catalogues. *Astronomy*, 65.

MathWorks-Inc. (2017). MATLAB version: 9.3 (R2017b). *The MathWorks Inc*. Retrieved from https://www.mathworks.com: https://www.mathworks.com

Melia, F., & Shevchuk, A. (2012). The Rh=ct Universe. *Mon. Not. R. Astron. Soc.*, 2579-2586.

Meszaros, A. (2019). An Oppositeness in the Cosmology: Distribution of the Gamma-Ray Bursts and the Cosmological Principle. *ArXiv: 1912.07523v1 [Astro-Ph]*, 1-6.

Miguelote, A., & Ribeiro, M. (1998). Fractals and the Distribution of Galaxies. *Brazilian Journal of Physics*, 1-29.

Milakovic, D., Lee, C., & Molaro, P. W. (2023). Methods for quasar absorption system measurements of the fine structure constant in the 2020s and beyond. *arXiv:2212.02458.*, 1-10.

Mohajan, H. (2013). Friedmann, Robertson- Walker (FRW) Models in Cosmology. *Journal of Environmental Treatment Techniques*, 2309-1185.

Mureika, J. (2007). Fractal Holography: a geometric re-interpretation of cosmological large scale structure. *Journal of Cosmology and Astroparticle Physics*, 1-9.

Mustapha, N., Hellaby, C., & Ellis, G. (1997). Large-scale inhomogeneity versus source evolution: Can we distinguish them observationally? *Monthly Notices of the Royal Astronomical Society*, 817-830.

Pandey, B., & Sarkar, S. (2016). Probing large scale homogeneity and periodicity in the LRG distribution using Shannon entropy. *Monthly Notices of the Royal Astronomical Society*, 1519-1528.

Paris, I., Petitjean, P., Ross, N., Myers, A., Aubourg, E., Streblyanska, A., . . . C., Y. (2017). The Sloan Digital Sky Survey Quasar Catalog: Twelfth data release. *Astronomy and Astrophysics*, A79.

Peebles. (1998). The Standard Cosmological Model. *ArXiv: Astro- Ph/9806201*, 1-18.

Pietronero, L., & Labini, F. (1996). Multifractality as a Link Between Luminosity and Space Distribution of Visible Matter. *The Astrophysical Journal*, 1-38.

Ribeiro, .M.B, (1993). On Modelling a Relativistic Hierarchical (Fractal) Cosmology by Tolman's Spacetime. II. Analysis of the Einstein-de Sitter Model. *Astrophys.J.*, 469-485.

Ribeiro, A., & Miguelote, M. (1998). Fractals and the Distribution of Galaxies. *Brazilian Journal of Physics*, 1-28.

Riess, A., Filippenko, A., Challis, P., Clocchiatti, A., Diercks, A., Garnavich, P., Kirshner, R. (1998). Observational evidence from supernovae for an accelerating universe and a cosmological constant. *Astron. J.*, 1009–1038.

Secrest, N., Hausegger, S., Rameez, M., Mohayaee, R., Sarkar, S., & Colin, J. (2021). A Test of the Cosmological Principle with Quasars. *Astrophys.J.Lett.*, 1-9.

Seshavatharam, U., & Lakshminarayana, S. (2023). A Rotating Model of a Light Speed Expanding Hubble-Hawking Universe. *Phys. Sci. Forum*, ECU2023-14065.

Shamir, L. (2024). A Simple Direct Empirical Observation of Systematic Bias of the Redshift as a Distance Indicator. *Astronomy*, 1-16.

Smith, N., Keivan, G., & Stassun. (2017). The Canonical Luminous Blue Variable AG Car and Its Neighbor Hen 3-519 Are much closer than previously assumed. *The Astronomical Journal*, 1199-1204.

Tian, S. (2017). The Relation between Cosmological Redshift and Scale Factor for Photons. *The Astrophysical Journal*, 1-5.

Wamalwa, D. (2016). On the Friedmann Cosmology. *International Journal of Pure and Applied Mathematics*, 803-818.

Werner, & Schermelleh, E. (2010). Deciding Between Competing Models: Chi-Square Difference Tests. *The Astrophysical Journal*, 1-3.

Wojtak, R., & Prada, F. (2017). Redshift remapping and cosmic acceleration in dark-matter-dominated cosmological models. *Monthly Notices of the Royal Astronomical Society*, 4493-4511.

York, D., Adelman, J., John, E., Anderson, J., Scott, F., Anderson., Bakken. (2000). The Sloan Digital Sky Survey: Technical Summary. *The Astronomical Journal*, 1199-1204.

APPENDIX

Appendix A

In the MATLAB codes, the following values have been used: redshift from $z = 0$ to $z = 5$, density of the Universe from $\rho(t_0) = 3\times 10^{-27}$ kgm^{-3} to $\rho(t_0) = 8.783 \times 10^{-25}$ kgm^{-3}, speed of light $c = 3 \times 10^8$ m/s, cosmic scale factor $R(t_0) = 9 \times 10^{25}$ m (but can be varied appropriately too), the gravitational constant $G = 6.67 \times 10^{-11}$ m^3 kg^{-1} s^{-2}, curvature scalar of the Universe $\kappa = -1, 0, 1$. In all specified modified redshift models, required parameter values are given that have been reconstructed from observational data hence they can be compared for same matter density and curvature. All the values used in our codes are in line with available statistics.

Appendix B

MATLAB codes for the model $f(z) = \alpha_1 z + \alpha_2 z^2$ with α_1=episilon1=2.005 and α_2 =episilon2 =0.005 and standard redshift for light intensity with redshift.

```
clc
clear
close all
% Case 1: k=0, Flat Universe
Figure(1) ;clf
rho = 3*10^(-27);
c = 3*10^8;  % speed of light
R = 9*10^25; % cosmic scale factor equal to value of R(to)
G = 6.67*10^-11; % Gravitational constant
z =0:0.0001:5;
L = 1;
kappa =0; % the curvature parameter of the universe, gives value of k
beta = 8*pi*G*c^-4;
alpha = rho*R^3;
a1 =beta*c^2*alpha-12*kappa*R;
a2 =((beta*c^2*alpha)*(1+z))-(12*kappa*R);
n1=((sqrt(12*R)*(sqrt(a2)-sqrt(a1)))./(sqrt(a1*a2)+(12*kappa*R))).^2;
n =L*(1+kappa*n1).^2; % Numerator
d0 = ((sqrt(12*R)*(sqrt(a2)-sqrt(a1)))./(sqrt(a1*a2)+(12*kappa*R))).^2;
d1 =4*pi*(1+z).^2*R.^2;
d = d0.*d1; % Denominator
I = log(n./d); % Gives values of intensity of light
plot(z,I,'b-','LineWidth',1)
xlabel('\fontname{Times New Roman}Redshift (z)','FontSize',12)
ylabel('\fontname{Times New Roman}Log(I)','FontSize',11)
title('\fontname{Times New Roman}Light intensity against redshift (z)','FontSize',12)
set(gca, 'XMinorTick','on', 'YMinorTick','on')
set(gca,'xtick',0:1:5)
set(gca, 'XMinorTick','on', 'YMinorTick','on')
hold on
% Case 2: k=-1, Open Universe
% Defining constants
rho = 5*10^-27; % Upper density of the universe
c = 3*10^8;  % speed of light
R = 9*10^25;  % cosmic scale factor equal to value of R(to)
G = 6.67*10^-11; % Gravitational constant
z =0:0.0001:5;
L = 1;
kappa=-1;  % the curvature parameter of the universe, gives value of k
beta = 8*pi*G*c^-4;
alpha = rho*R^3;
a1 =(beta*c^2*alpha)-(12*kappa*R);
a2 =((beta*c^2*alpha)*(1+z))-(12*kappa*R);
n1=((sqrt(12*R)*(sqrt(a2)-sqrt(a1)))./(sqrt(a1*a2)+(12*kappa*R))).^2;
n =L*(1+kappa*n1).^2; % Numerator
d0 = ((sqrt(12*R)*(sqrt(a2)-sqrt(a1)))./(sqrt(a1*a2)+(12*kappa*R))).^2;
d1 =(4*pi*(1+z).^2)*R.^2;
d = d0.*d1; % Denominator
I = log(n./d);% Gives values of intensity of light
plot(z,I,'g-','LineWidth',1)
% Case 3: k=+1, Closed Universe
% Defining constants
rho = 8.78*10^-25; % Upper density of the universe
c = 3*10^8;  % speed of light
R = 9*10^25;  % cosmic scale factor equal to value of R(to)
G = 6.67*10^-11; % Gravitational constant
z =0:0.0001:5;
L = 1;
kappa=1;  % the curvature parameter of the universe, gives value of k
beta = 8*pi*G*c^-4;
alpha = rho*R^3;
a1 =(beta*c^2*alpha)-(12*kappa*R);
a2 = ((beta*c^2*alpha)*(1+z))-(12*kappa*R);
n1=((sqrt(12*R)*(sqrt(a2)-sqrt(a1)))./(sqrt(a1*a2)+(12*kappa*R))).^2;
n =L*(1+kappa*n1).^2; % Numerator
d0 = ((sqrt(12*R)*(sqrt(a2)-sqrt(a1)))./(sqrt(a1*a2)+(12*kappa*R))).^2;
```

```
d1 =(4*pi*(1+z).^2)*R.^2;
d = d0.*d1; % Denominator
I = log(n./d); % Gives values of intensity of light
plot(z,I,'r-','LineWidth',1)
legend('\rho= 3 × 10^{−27}, \kappa= 0','\rho=5 × 10^{−27}, \kappa= −1','\rho= 8.78 ×
10^{−25}, \kappa= 1','Location','NorthEast')
% modified models
% Case 1: k=0, Flat Universe
rho = 3*10^-27;
c = 3*10^8;  % speed of light
R = 9*10^25;  % cosmic scale factor equal to value of R(to)
G = 6.67*10^-11; % Gravitational constant
z =0:0.0001:5;
L = 1;
epsilon1 = 2.005;
epsilon2 = 0.005;
kappa = 0;  % the curvature parameter of the universe, gives value of k
beta = 8*pi*G*c^-4;
alpha = rho*R^3;
a1 =(beta*c^2*alpha)-(12*kappa*R);
a2 =((beta*c^2*alpha)*(1+epsilon1*z+epsilon2*z.^2))-(12*kappa*R);
n1=((sqrt(12*R)*(sqrt(a2)-sqrt(a1)))./(sqrt(a1*a2)+(12*kappa*R))).^2;
n =L*(1+kappa*n1).^2; % Numerator
d0 =(sqrt(12*R)*(sqrt(a2)-sqrt(a1))./(sqrt(a1*a2)+(12*kappa*R))).^2;
d1 =4*pi*(1+epsilon1*z+epsilon2*z.^2).^2 *R.^2;
d = d0.*d1; % Denominator
I = log(n./d); % Gives values of intensity of light
plot(z,I,':b','LineWidth',1)
% Case 2: k=-1, Open Universe
rho = 5*10^-27;
c = 3*10^8;  % speed of light
R = 9*10^25; % cosmic scale factor equal to value of R(to)
G = 6.67*10^-11; % Gravitational constant
z =0:0.0001:5;
L = 1;
epsilon1 = 2.005;
epsilon2 = 0.005;
kappa = -1;% the curvature parameter of the universe, gives value of k
beta = 8*pi*G*c^-4;
alpha = rho*R^3;
a1 = ((beta*c^2*alpha)-(12*kappa*R));
a2 = ((beta*c^2*alpha)*(1+epsilon1*z+epsilon2*z.^2))-(12*kappa*R);
n1=(sqrt(12*R)*(sqrt(a2)-sqrt(a1)))./(sqrt(a1*a2)+(12*kappa*R))).^2;
n =L*(1+kappa*n1).^2; % Numerator
d0 = (sqrt(12*R)*(sqrt(a2)-sqrt(a1))./(sqrt(a1*a2)+(12*kappa*R))).^2;
d1 =4*pi*(1+epsilon1*z+epsilon2*z.^2).^2 *R.^2;
d = d0.*d1; % Denominator
I = log(n./d); % Gives values of intensity of light
plot(z,I,':g','LineWidth',1)
% Case 3: k=+1, Closed Universe
rho = 8.78*10^-25;
c = 3*10^8;  % speed of light
R = 9*10^25;% cosmic scale factor equal to value of R(to)
G = 6.67*10^-11; % Gravitational constant
z =0:0.0001:5;
L = 1;
epsilon1 = 2.005;
epsilon2 = 0.005;
kappa =1;% the curvature parameter of the universe, gives value of k
beta = 8*pi*G*c^-4;
alpha = rho*R^3;
a1 = (beta*c^2*alpha)-(12*kappa*R);
a2 = ((beta*c^2*alpha)*(1+epsilon1*z+epsilon2*z.^2))-(12*kappa*R);
n1=(sqrt(12*R)*(sqrt(a2)-sqrt(a1)))./(sqrt(a1*a2)+(12*kappa*R))).^2;
n =L*(1+kappa*n1).^2; % Numerator
d0 = (sqrt(12*R)*(sqrt(a2)-sqrt(a1))./(sqrt(a1*a2)+(12*kappa*R))).^2;
d1 =4*pi*(1+epsilon1*z+epsilon2*z.^2).^2 *R.^2;
d = d0.*d1; % Denominator
I = log(n./d); % Gives values of intensity of light
plot(z,I,':r','LineWidth',1)
hold off
```

Appendix C

MATLAB codes for the model $f(z) = z + \gamma(z)^2$, where $\gamma(z)$ is a free function of z with $\gamma =$ episilon = 0.45 and the standard redshift for light intensity with redshift.

```
clc
clear
close all
% Case 1: k=0, Flat Universe
Figure(1) ;clf
rho = 3*10^(-27);
c = 3*10^8;  % speed of light
R = 9*10^25; % cosmic scale factor equal to value of R(to)
G = 6.67*10^-11; % Gravitational constant
z =0:0.0001:5;
L = 1;
kappa = 0;% the curvature parameter of the universe, gives value of k
beta = 8*pi*G*c^-4;
alpha = rho*R^3;
a1 =beta*c^2*alpha-12*kappa*R;
a2 =((beta*c^2*alpha)*(1+z))-(12*kappa*R);
n1=((sqrt(12*R)*(sqrt(a2)-sqrt(a1)))./(sqrt(a1*a2)+(12*kappa*R))).^2;
n =L*(1+kappa*n1).^2; % Numerator
d0 = ((sqrt(12*R)*(sqrt(a2)-sqrt(a1)))./(sqrt(a1*a2)+(12*kappa*R))).^2;
d1 =4*pi*(1+z).^2*R.^2;
d = d0.*d1; % Denominator
I = log(n./d); % Gives values of intensity of light
plot(z,I,'b-','LineWidth',1)
xlabel('\fontname{Times New Roman}Redshift (z)','FontSize',12)
ylabel('\fontname{Times New Roman}Log(I)','FontSize',11)
title('\fontname{Times New Roman}Light intensity against redshift (z)','FontSize',12)
set(gca, 'XMinorTick','on', 'YMinorTick','on')
set(gca,'xtick',0:1:5)
set(gca, 'XMinorTick','on', 'YMinorTick','on')
hold on
% Case 2: k=-1, Open Universe
% Defining constants
rho = 5*10^-27; % Upper density of the universe
c = 3*10^8;  % speed of light
R = 9*10^25;  % cosmic scale factor equal to value of R(to)
G = 6.67*10^-11;% Gravitational constant
z =0:0.0001:5;
L = 1;
kappa=-1; % the curvature parameter of the universe,gives value of k
beta = 8*pi*G*c^-4;
alpha = rho*R^3;
a1 =(beta*c^2*alpha)-(12*kappa*R);
a2 =((beta*c^2*alpha)*(1+z))-(12*kappa*R);
n1=((sqrt(12*R)*(sqrt(a2)-sqrt(a1)))./(sqrt(a1*a2)+(12*kappa*R))).^2;
n =L*(1+kappa*n1).^2; % Numerator
d0 = ((sqrt(12*R)*(sqrt(a2)-sqrt(a1)))./(sqrt(a1*a2)+(12*kappa*R))).^2;
d1 =(4*pi*(1+z).^2)*R.^2;
d = d0.*d1; % Denominator
I = log(n./d);% Gives values of intensity of light
plot(z,I,'g-','LineWidth',1)
% Case 3: k=+1, Closed Universe
% Defining constants
rho = 8.78*10^-25; % Upper density of the universe
c = 3*10^8;  % speed of light
R = 9*10^25;  % cosmic scale factor equal to value of R(to)
G = 6.67*10^-11; % Gravitational constant
z =0:0.0001:5;
L = 1;
kappa=1;  % the curvature parameter of the universe, gives value of k
beta = 8*pi*G*c^-4;
alpha = rho*R^3;
a1 =(beta*c^2*alpha)-(12*kappa*R);
a2 = ((beta*c^2*alpha)*(1+z))-(12*kappa*R);
n1=((sqrt(12*R)*(sqrt(a2)-sqrt(a1)))./(sqrt(a1*a2)+(12*kappa*R))).^2;
```

```
n =L*(1+kappa*n1).^2; % Numerator
d0 = ((sqrt(12*R)*(sqrt(a2)-sqrt(a1))./(sqrt(a1*a2)+(12*kappa*R))).^2;
d1 =(4*pi*(1+z).^2)*R.^2;
d = d0.*d1; % Denominator
I = log(n./d); % Gives values of intensity of light
plot(z,I,'r-','LineWidth',1)
legend('\rho= 3 × 10^{−27}, \kappa= 0','\rho=5 × 10^{−27}, \kappa= −1','\rho= 8.78 ×
10^{−25}, \kappa= 1','Location','NorthEast')
% modified model
% Case 1: k=0, Flat Universe
rho = 3*10^-27;
c = 3*10^8;  % speed of light
R = 9*10^25;  % cosmic scale factor equal to value of R(to)
G = 6.67*10^-11; % Gravitational constant
z =0:0.0001:5;
L = 1;
epsilon = 0.45;
kappa = 0;  % the curvature parameter of the universe, gives value of k
beta = 8*pi*G*c^-4;
alpha = rho*R^3;
a1 =(beta*c^2*alpha)-(12*kappa*R);
a2 =((beta*c.^2*alpha)*(1+z+epsilon*z.^2))-12*kappa*R;
n1=((sqrt(12*R)*(sqrt(a2)-sqrt(a1))./(sqrt(a1*a2)+(12*kappa*R))).^2;
n =L*(1+kappa*n1).^2; % Numerator
d0 =(sqrt(12*R)*(sqrt(a2)-sqrt(a1))./(sqrt(a1*a2)+(12*kappa*R))).^2;
d1 =4*pi*(1+z+epsilon*z.^2).^2 *R.^2;
d = d0.*d1; % Denominator
I = log(n./d); % Gives values of intensity of light
plot(z,I,':b','LineWidth',1)
% Case 2: k=-1, Open Universe
rho = 5*10^-27;
c = 3*10^8;  % speed of light
R = 9*10^25; % cosmic scale factor equal to value of R(to)
G = 6.67*10^-11; % Gravitational constant
z =0:0.0001:5;
L = 1;
epsilon = 0.45;
kappa = -1; %the curvature parameter of the universe, gives value of k
beta = 8*pi*G*c^-4;
alpha = rho*R^3;
a1 = ((beta*c^2*alpha)-(12*kappa*R));
a2 =((beta*c.^2*alpha)*(1+z+epsilon*z.^2))-12*kappa*R;
n1=(sqrt(12*R)*(sqrt(a2)-sqrt(a1))./(sqrt(a1*a2)+(12*kappa*R))).^2;
n =L*(1+kappa*n1).^2; % Numerator
d0 = (sqrt(12*R)*(sqrt(a2)-sqrt(a1))./(sqrt(a1*a2)+(12*kappa*R))).^2;
d1 =4*pi*(1+z+epsilon*z.^2).^2 *R.^2;
d = d0.*d1; % Denominator
I = log(n./d); % Gives values of intensity of light
plot(z,I,':g','LineWidth',1)
% Case 3: k=+1,Closed Universe
rho = 8.78*10^-25;
c = 3*10^8;  % speed of light
R = 9*10^25;% cosmic scale factor equal to value of R(to)
G = 6.67*10^-11; % Gravitational constant
z =0:0.0001:5;
L = 1;
epsilon = 0.45;
kappa =1;% the curvature parameter of the universe, gives value of k
beta = 8*pi*G*c^-4;
alpha = rho*R^3;
a1 = (beta*c^2*alpha)-(12*kappa*R);
a2 =((beta*c.^2*alpha)*(1+z+epsilon*z.^2))-12*kappa*R;
n1=(sqrt(12*R)*(sqrt(a2)-sqrt(a1))./(sqrt(a1*a2)+(12*kappa*R))).^2;
n =L*(1+kappa*n1).^2; % Numerator
d0 = (sqrt(12*R)*(sqrt(a2)-sqrt(a1))./(sqrt(a1*a2)+(12*kappa*R))).^2;
d1 =4*pi*(1+z+epsilon*z.^2).^2 *R.^2;
d = d0.*d1; % Denominator
I = log(n./d); % Gives values of intensity of light
plot(z,I,':r','LineWidth',1)
hold off
```

Appendix D

MATLAB codes for the modified redshift $(z) = \frac{z}{\varepsilon}$, with $\varepsilon = 0.45$ and the standard redshift model for light intensity with redshift.

```
clc
clear
close all
% Case 1: k=0, Flat Universe
Figure(1) ;clf
rho = 3*10^(-27);
c = 3*10^8;  % speed of light
R = 9*10^25; % cosmic scale factor equal to value of R(to)
G = 6.67*10^-11; % Gravitational constant
z =0:0.0001:5;
L = 1;
kappa = 0; % the curvature parameter of the universe, gives value of k
beta = 8*pi*G*c^-4;
alpha = rho*R^3;
a1 =beta*c^2*alpha-12*kappa*R;
a2 =((beta*c^2*alpha)*(1+z))-(12*kappa*R);
n1=((sqrt(12*R)*(sqrt(a2)-sqrt(a1)))./(sqrt(a1*a2)+(12*kappa*R))).^2;
n =L*(1+kappa*n1).^2; % Numerator
d0 = ((sqrt(12*R)*(sqrt(a2)-sqrt(a1)))./(sqrt(a1*a2)+(12*kappa*R))).^2;
d1 =4*pi*(1+z).^2*R.^2;
d = d0.*d1; % Denominator
I = log(n./d); % Gives values of intensity of light
plot(z,I,'b-','LineWidth',1)
xlabel('\fontname{Times New Roman}Redshift (z)','FontSize',12)
ylabel('\fontname{Times New Roman}Log(I)','FontSize',11)
title('\fontname{Times New Roman}Light intensity against redshift (z)','FontSize',12)
set(gca, 'XMinorTick','on', 'YMinorTick','on')
set(gca,'xtick',0:1:5)
set(gca, 'XMinorTick','on', 'YMinorTick','on')
hold on
% Case 2: k=-1, Open Universe
% Defining constants
rho = 5*10^-27; % Upper density of the universe
c = 3*10^8;  % speed of light
R = 9*10^25;  % cosmic scale factor equal to value of R(to)
G = 6.67*10^-11; % Gravitational constant
z =0:0.0001:5;
L = 1;
kappa=-1;  % the curvature parameter of the universe, gives value of k
beta = 8*pi*G*c^-4;
alpha = rho*R^3;
a1 =(beta*c^2*alpha)-(12*kappa*R);
a2 =((beta*c^2*alpha)*(1+z))-(12*kappa*R);
n1=((sqrt(12*R)*(sqrt(a2)-sqrt(a1)))./(sqrt(a1*a2)+(12*kappa*R))).^2;
n =L*(1+kappa*n1).^2; % Numerator
d0 = ((sqrt(12*R)*(sqrt(a2)-sqrt(a1)))./(sqrt(a1*a2)+(12*kappa*R))).^2;
d1 =(4*pi*(1+z).^2)*R.^2;
d = d0.*d1; % Denominator
I = log(n./d);% Gives values of intensity of light
plot(z,I,'g-','LineWidth',1)
% Case 3: k=+1, Closed Universe
% Defining constants
rho = 8.78*10^-25; % Upper density of the universe
c = 3*10^8;  % speed of light
R = 9*10^25;  % cosmic scale factor equal to value of R(to)
G = 6.67*10^-11; % Gravitational constant
z =0:0.0001:5;
L = 1;
kappa=1;  % the curvature parameter of the universe, gives value of k
beta = 8*pi*G*c^-4;
alpha = rho*R^3;
a1 =(beta*c^2*alpha)-(12*kappa*R);
a2 = ((beta*c^2*alpha)*(1+z))-(12*kappa*R);
n1=((sqrt(12*R)*(sqrt(a2)-sqrt(a1)))./(sqrt(a1*a2)+(12*kappa*R))).^2;
```

```
n =L*(1+kappa*n1).^2; % Numerator
d0 = ((sqrt(12*R)*(sqrt(a2)-sqrt(a1))./(sqrt(a1*a2)+(12*kappa*R))).^2;
d1 =(4*pi*(1+z).^2)*R.^2;
d = d0.*d1; % Denominator
I = log(n./d); % Gives values of intensity of light
plot(z,I,'r-','LineWidth',1)
legend('\rho= 3 × 10^{−27}, \kappa= 0','\rho=5 × 10^{−27}, \kappa= −1','\rho= 8.78 ×
10^{−25}, \kappa= 1','Location','NorthEast')
% modified models
% Case 1: k=0, Flat Universe
rho = 3*10^-27;
c = 3*10^8;  % speed of light
R = 9*10^25;  % cosmic scale factor equal to value of R(to)
G = 6.67*10^-11; % Gravitational constant
z =0:0.0001:5;
L = 1;
epsilon = 0.45;
kappa = 0;  % the curvature parameter of the universe, gives value of k
beta = 8*pi*G*c^-4;
alpha = rho*R^3;
a1 =(beta*c^2*alpha)-(12*kappa*R);
a2 =(beta*c^2*alpha)*(1+z./epsilon)-(12*kappa*R);
n1=((sqrt(12*R)*(sqrt(a2)-sqrt(a1)))./(sqrt(a1*a2)+(12*kappa*R))).^2;
n =L*(1+kappa*n1).^2; % Numerator
d0 =(sqrt(12*R)*(sqrt(a2)-sqrt(a1))./(sqrt(a1*a2)+(12*kappa*R))).^2;
d1 =4*pi*(1+z./epsilon).^2 *R.^2;
d = d0.*d1; % Denominator
I = log(n./d); % Gives values of intensity of light
plot(z,I,':b','LineWidth',1)
% Case 2: k=-1, Open Universe
rho = 5*10^-27;
c = 3*10^8;  % speed of light
R = 9*10^25; % cosmic scale factor equal to value of R(to)
G = 6.67*10^-11; % Gravitational constant
z =0:0.0001:5;
L = 1;
epsilon = 0.45;
kappa = -1;  % the curvature parameter of the universe, gives value of k
beta = 8*pi*G*c^-4;
alpha = rho*R^3;
a1 = ((beta*c^2*alpha)-(12*kappa*R));
a2 =(beta*c^2*alpha)*(1+z./epsilon)-(12*kappa*R);
n1=(sqrt(12*R)*(sqrt(a2)-sqrt(a1))./(sqrt(a1*a2)+(12*kappa*R))).^2;
n =L*(1+kappa*n1).^2; % Numerator
d0 = (sqrt(12*R)*(sqrt(a2)-sqrt(a1))./(sqrt(a1*a2)+(12*kappa*R))).^2;
d1 =4*pi*(1+z./epsilon).^2 *R.^2;
d = d0.*d1; % Denominator
I = log(n./d); % Gives values of intensity of light
plot(z,I,':g','LineWidth',1)
% Case 3: k=+1, Closed Universe
rho = 8.78*10^-25;
c = 3*10^8;  % speed of light
R = 9*10^25;% cosmic scale factor equal to value of R(to)
G = 6.67*10^-11; % Gravitational constant
z =0:0.0001:5;
L = 1;
epsilon = 0.45;
kappa =1;  % the curvature parameter of the universe, gives value of k
beta = 8*pi*G*c^-4;
alpha = rho*R^3;
a1 = (beta*c^2*alpha)-(12*kappa*R);
a2 =(beta*c^2*alpha)*(1+z./epsilon)-(12*kappa*R);
n1=(sqrt(12*R)*(sqrt(a2)-sqrt(a1))./(sqrt(a1*a2)+(12*kappa*R))).^2;
n =L*(1+kappa*n1).^2; % Numerator
d0 = (sqrt(12*R)*(sqrt(a2)-sqrt(a1))./(sqrt(a1*a2)+(12*kappa*R))).^2;
d1 =4*pi*(1+z./epsilon).^2 *R.^2;
d = d0.*d1; % Denominator
I = log(n./d); % Gives values of intensity of light
plot(z,I,':r','LineWidth',1)
hold off
```

Appendix E

MATLAB code for the model $f(z) = \alpha_1 z + \alpha_2 z^2$ with α_1 =episilon1= 2.005 and α_2 =episilon2= 0.005 and standard redshift model for the number density with redshift.

```
clc
clear
close all
% Case 1: k=0, Flat
Figure(1);clf
z= 0:0.0001:5;
% Defining constants
rho = 3*10^-27; % Upper density of the universe
c = 3*10^8;  % speed of light
kappa =0; % Gives the value of k
R = 9*10^25; % cosmic scale factor, equal to value of R(to)
G = 6.67*10^-11; % Gravitational constant
N = 1; % Number of galaxies per unit volume
beta = 8*pi*G*c^-4; % Gives the value of beta
alpha = rho*R^3;
a = beta*c^2*alpha-12*kappa*R;
b = ((beta*c^2*alpha)*(1+z))-12*kappa*R;
n0 = 48*pi*N*R*(beta*c.^2*alpha).^2 *sqrt(3*R)*(sqrt(b)-sqrt(a)).^2;%numerator
d0 = (1+kappa*((sqrt(b)-sqrt(a))./(sqrt(a*b)+12*kappa*R)).^2).^3;
d1 = (sqrt(a*b)+12*kappa*R).^4;
d = d0.*d1; % Denominator
n=log(n0./d);
plot(z,n,'-b','LineWidth',1)
xlabel('\fontname{Times New Roman}Redshift (z)','FontSize',12)
ylabel('\fontname{Times New Roman}Log(n)','FontSize',12)
title('\fontname{Times New Roman} Number density against redshift (z)','FontSize',12)
set(gca,'xtick',0:1:5)
set(gca, 'XMinorTick','on', 'YMinorTick','on')
hold on
% Case 2: k=-1, Open
z = 0:0.0001:5;
% Defining constants
rho = 5*10^-27; % Upper density of the universe
c = 3*10^8;  % speed of light
kappa =-1; % Gives the value of k
R = 9*10^25; % cosmic scale factor, equal to value of R(to)
G = 6.67*10^-11; % Gravitational constant
N = 1; % Number of galaxies per unit volume
beta = 8*pi*G*c^-4; % Gives the value of beta
alpha = rho*R^3;
a = beta*c.^2*alpha-12*kappa*R;
b = ((beta*c.^2*alpha)*(1+z))-12*kappa*R;
n0 = 48*pi*N*R*(beta*c.^2*alpha).^2 *sqrt(3*R)*(sqrt(b)-sqrt(a)).^2;%numerator
d0 = (1+kappa*((sqrt(b)-sqrt(a))./(sqrt(a*b)+12*kappa*R)).^2).^3;
d1 = (sqrt(a*b)+12*kappa*R).^4;
d = d0.*d1; % Denominator
n=log(n0./d);
plot(z,n,'-g','LineWidth',1)
% Case 3: k=1, Closed
z = 0:0.0001:5;
% Defining constants
rho = 8.78*10^-25; % Upper density of the universe
c = 3*10^8;  % speed of light
kappa =1; % Gives the value of k
R = 9*10^25; % cosmic scale factor, equal to value of R(to)
G = 6.67*10^-11; % Gravitational constant
N = 1; % Number of galaxies per unit volume
beta = 8*pi*G*c^-4; % Gives the value of beta
alpha = rho*R^3;
a =(beta*c.^2*alpha)-12*kappa*R;
b =((beta*c.^2*alpha)*(1+z))-12*kappa*R;
n0 =48*pi*N*R*(beta*c.^2*alpha).^2 *sqrt(3*R)*(sqrt(b)-sqrt(a)).^2;%numerator
d0 =(1+kappa*((sqrt(b)-sqrt(a))./(sqrt(a*b)+12*kappa*R)).^2).^3;
d1 =(sqrt(a*b)+12*kappa*R).^4;
```

```
d = d0.*d1; % Denominator
n=log(n0./d);
plot(z,n,'-r','LineWidth',1)
legend('\rho=3 × 10^{−27}, \kappa= 0','\rho=5 × 10^{−27}, \kappa= −1 ','\rho= 8.78 ×
10^{−25}, \kappa= 1 ','Location','SouthEast')
% Modified model
% Case 1: k=0, Flat
z = 0:0.001:5;
% Defining constants
rho = 3*10^-27; % Upper density of the universe
c = 3*10^8;  % speed of light
kappa =0; % Gives the value of k
epsilon1 = 2.005;
epsilon2 = 0.005;
R = 9*10^25; % cosmic scale factor, equal to value of R(to)
G = 6.67*10^-11; % Gravitational constant
N = 1; % Number of galaxies per unit volume
beta = 8*pi*G*c^-4; % Gives the value of beta
alpha = rho*R^3;
a1 =(beta*c.^2*alpha)-(12*kappa*R);
a2 =((beta*c^2*alpha)*(1+epsilon1*z+epsilon2*z.^2))-(12*kappa*R);
n0 =48*pi*N*R*(beta*c.^2*alpha).^2*sqrt(3*R)*(sqrt(a2)-sqrt(a1)).^2;%numerator
d0 =(1+kappa *((sqrt(a2)-sqrt(a1))./(sqrt(a1*a2)+12*kappa*R)).^2).^3;
d1 =(sqrt(a1*a2)+12*kappa*R).^4;
d = d1.*d0; % Denominator
n=log(n0./d);
plot(z,n,':b','LineWidth',1)
% Case 2: k=-1, Open
z = 0:0.001:5;
% Defining constants
rho = 5*10^-27; % Upper density of the universe
c = 3*10.^8;  % speed of light
kappa =-1; % Gives the value of k
epsilon1 = 2.005;
epsilon2 = 0.005;
R = 9*10^25; % cosmic scale factor, equal to value of R(to)
G = 6.67*10^-11; % Gravitational constant
N = 1; % Number of galaxies per unit volume
beta = 8*pi*G*c^-4; % Gives the value of beta
alpha=rho*R^3;
a1 = (beta*c.^2*alpha)-12*kappa*R;
a2 = ((beta*c^2*alpha)*(1+epsilon1*z+epsilon2*z.^2))-(12*kappa*R);
n0 = 48*pi*N*R*(beta*c.^2*alpha).^2*sqrt(3*R)*(sqrt(a2)-sqrt(a1)).^2;%numerator
d0 = (1+kappa *((sqrt(a2)-sqrt(a1))./(sqrt(a1*a2)+12*kappa*R)).^2).^3;
d1 = (sqrt(a1*a2)+12*kappa*R).^4;
d = d1.*d0; % Denominator
n=log(n0./d);
plot(z,n,':g','LineWidth',1)
% Case 3: k=+1, Closed Universe = 0:0.001:5;
% Defining constants
rho = 8.78*10^-25; % Upper density of the universe
c = 3*10.^8;  % speed of light
kappa =1; % Gives the value of k
epsilon1 = 2.005;
epsilon2 = 0.005;
R = 9*10^25; % cosmic scale factor, equal to value of R(to)
G = 6.67*10^-11; % Gravitational constant
N = 1; % Number of galaxies per unit volume
beta = 8*pi*G*c^-4; % Gives the value of beta
alpha = rho*R^3;
a1 =(beta*c.^2*alpha)-(12*kappa*R);
a2 =((beta*c^2*alpha)*(1+epsilon1*z+epsilon2*z.^2))-(12*kappa*R);
n0 =48*pi*N*R*(beta*c.^2*alpha).^2*sqrt(3*R)*(sqrt(a2)-sqrt(a1)).^2;%numerator
d0 =(1+kappa*((sqrt(a2)-sqrt(a1))./(sqrt(a1*a2)+12*kappa*R)).^2).^3;
d1 =(sqrt(a1*a2)+12*kappa*R).^4;
d = d1.*d0; % Denominator
n=log(n0./d);
plot(z,n,':r','LineWidth',1)
hold off
```

Appendix F

MATLAB codes for the modified redshift $f(z) = z + \gamma(z)^2$, where $\gamma(z)$ is a free function of z with γ =episilon=0.45 and the standard redshift for number density with redshift.

```
clc
clear
close all
% Case 1: k=0, Flat
Figure(1);clf
z= 0:0.0001:5;
% Defining constants
rho = 3*10^-27; % Upper density of the universe
c = 3*10^8;  % speed of light
kappa =0; % Gives the value of k
R = 9*10^25; % cosmic scale factor, equal to value of R(to)
G = 6.67*10^-11; % Gravitational constant
N = 1; % Number of galaxies per unit volume
beta = 8*pi*G*c^-4; % Gives the value of beta
alpha = rho*R^3;
a = beta*c^2*alpha-12*kappa*R;
b = ((beta*c^2*alpha)*(1+z))-12*kappa*R;
n0 = 48*pi*N*R*(beta*c.^2*alpha).^2 *sqrt(3*R)*(sqrt(b)-sqrt(a)).^2;%numerator
d0 = (1+kappa*((sqrt(b)-sqrt(a))./(sqrt(a*b)+12*kappa*R)).^2).^3;
d1 = (sqrt(a*b)+12*kappa*R).^4;
d = d0.*d1; % Denominator
n=log(n0./d);
plot(z,n,'-b','LineWidth',1)
xlabel('\fontname{Times New Roman}Redshift (z)','FontSize',12)
ylabel('\fontname{Times New Roman}Log(n)','FontSize',12)
title('\fontname{Times New Roman} Number density against redshift (z)','FontSize',12)
set(gca,'xtick',0:1:5)
set(gca, 'XMinorTick','on', 'YMinorTick','on')
hold on
% Case 2: k=-1, Open
z = 0:0.0001:5;
% Defining constants
rho = 5*10^-27; % Upper density of the universe
c = 3*10^8;  % speed of light
kappa =-1; % Gives the value of k
R = 9*10^25; % cosmic scale factor, equal to value of R(to)
G = 6.67*10^-11; % Gravitational constant
N = 1; % Number of galaxies per unit volume
beta = 8*pi*G*c^-4; % Gives the value of beta
alpha = rho*R^3;
a = beta*c.^2*alpha-12*kappa*R;
b = ((beta*c.^2*alpha)*(1+z))-12*kappa*R;
n0 = 48*pi*N*R*(beta*c.^2*alpha).^2 *sqrt(3*R)*(sqrt(b)-sqrt(a)).^2;%numerator
d0 = (1+kappa*((sqrt(b)-sqrt(a))./(sqrt(a*b)+12*kappa*R)).^2).^3;
d1 = (sqrt(a*b)+12*kappa*R).^4;
d = d0.*d1; % Denominator
n=log(n0./d);
plot(z,n,'-g','LineWidth',1)
% Case 3: k=1, Closed
z = 0:0.0001:5;
% Defining constants
rho = 8.78*10^-25; % Upper density of the universe
c = 3*10^8;  % speed of light
kappa =1; % Gives the value of k
R = 9*10^25; % cosmic scale factor, equal to value of R(to)
G = 6.67*10^-11; % Gravitational constant
N = 1; % Number of galaxies per unit volume
beta = 8*pi*G*c^-4; % Gives the value of beta
alpha = rho*R^3;
a =(beta*c.^2*alpha)-12*kappa*R;
b =((beta*c.^2*alpha)*(1+z))-12*kappa*R;
n0 =48*pi*N*R*(beta*c.^2*alpha).^2 *sqrt(3*R)*(sqrt(b)-sqrt(a)).^2;%numerator
d0 =(1+kappa*((sqrt(b)-sqrt(a))./(sqrt(a*b)+12*kappa*R)).^2).^3;
d1 =(sqrt(a*b)+12*kappa*R).^4;
```

```
d = d0.*d1; % Denominator
n=log(n0./d);
plot(z,n,'-r','LineWidth',1)
legend('\rho=3 × 10^{−27}, \kappa= 0','\rho=5 × 10^{−27}, \kappa= −1 ','\rho= 8.78 ×
10^{−25}, \kappa= 1 ','Location','SouthEast')
% Modified model
% Case 1: k=0, Flat
z = 0:0.001:5;
% Defining constants
rho = 3*10^-27; % Upper density of the universe
c = 3*10^8;  % speed of light
kappa =0; % Gives the value of k
epsilon = 0.45;
R = 9*10^25; % cosmic scale factor, equal to value of R(to)
G = 6.67*10^-11; % Gravitational constant
N = 1; % Number of galaxies per unit volume
beta = 8*pi*G*c^-4; % Gives the value of beta
alpha = rho*R^3;
a1 =(beta*c.^2*alpha)-(12*kappa*R);
a2 =((beta*c^2*alpha)*(1+z+epsilon*z.^2))-(12*kappa*R);
n0 =48*pi*N*R*(beta*c.^2*alpha).^2*sqrt(3*R)*(sqrt(a2)-sqrt(a1)).^2;%numerator
d0 =(1+kappa *((sqrt(a2)-sqrt(a1))./(sqrt(a1*a2)+12*kappa*R)).^2).^3;
d1 =(sqrt(a1*a2)+12*kappa*R).^4;
d = d1.*d0; % Denominator
n=log(n0./d);
plot(z,n,':b','LineWidth',1)
% Case 2: k=-1, Open
z = 0:0.001:5;
% Defining constants
rho = 5*10^-27; % Upper density of the universe
c = 3*10.^8;  % speed of light
kappa =-1; % Gives the value of k
epsilon = 0.45;
R = 9*10^25; % cosmic scale factor, equal to value of R(to)
G = 6.67*10^-11; % Gravitational constant
N = 1; % Number of galaxies per unit volume
beta = 8*pi*G*c^-4; % Gives the value of beta
alpha=rho*R^3;
a1 = (beta*c.^2*alpha)-12*kappa*R;
a2 = ((beta*c^2*alpha)*(1+z+epsilon*z.^2))-(12*kappa*R);
n0 = 48*pi*N*R*(beta*c.^2*alpha).^2*sqrt(3*R)*(sqrt(a2)-sqrt(a1)).^2;%numerator
d0 = (1+kappa *((sqrt(a2)-sqrt(a1))./(sqrt(a1*a2)+12*kappa*R)).^2).^3;
d1 = (sqrt(a1*a2)+12*kappa*R).^4;
d = d1.*d0; % Denominator
n=log(n0./d);
plot(z,n,':g','LineWidth',1)
% Case 3: k=+1, Closed Universe = 0:0.001:5;
% Defining constants
rho = 8.78*10^-25; % Upper density of the universe
c = 3*10.^8;  % speed of light
kappa =1; % Gives the value of k
R = 9*10^25; % cosmic scale factor, equal to value of R(to)
G = 6.67*10^-11; % Gravitational constant
N = 1; % Number of galaxies per unit volume
epsilon = 0.45;
beta = 8*pi*G*c^-4; % Gives the value of beta
alpha = rho*R^3;
a1 =(beta*c.^2*alpha)-(12*kappa*R);
a2 =((beta*c^2*alpha)*(1+z+epsilon*z.^2))-(12*kappa*R);
n0 =48*pi*N*R*(beta*c.^2*alpha).^2*sqrt(3*R)*(sqrt(a2)-sqrt(a1)).^2;%numerator
d0 =(1+kappa*((sqrt(a2)-sqrt(a1))./(sqrt(a1*a2)+12*kappa*R)).^2).^3;
d1 =(sqrt(a1*a2)+12*kappa*R).^4;
d = d1.*d0; % Denominator
n=log(n0./d);
plot(z,n,':r','LineWidth',1)
hold off
```

Appendix G

MATLAB codes for the modified redshift $(z) = \frac{z}{\varepsilon}$, with $\varepsilon = 0.45$ and the standard redshift model for number density with redshift.

```
clc
clear
close all
% Case 1: k=0, Flat
Figure(1);clf
z= 0:0.0001:5;
% Defining constants
rho = 3*10^-27; % Upper density of the universe
c = 3*10^8;  % speed of light
kappa =0; % Gives the value of k
R = 9*10^25; % cosmic scale factor, equal to value of R(to)
G = 6.67*10^-11; % Gravitational constant
N = 1; % Number of galaxies per unit volume
beta = 8*pi*G*c^-4; % Gives the value of beta
alpha = rho*R^3;
a = beta*c^2*alpha-12*kappa*R;
b = ((beta*c^2*alpha)*(1+z))-12*kappa*R;
n0 = 48*pi*N*R*(beta*c.^2*alpha).^2 *sqrt(3*R)*(sqrt(b)-sqrt(a)).^2;%numerator
d0 = (1+kappa*((sqrt(b)-sqrt(a))./(sqrt(a*b)+12*kappa*R)).^2).^3;
d1 = (sqrt(a*b)+12*kappa*R).^4;
d = d0.*d1; % Denominator
n=log(n0./d);
plot(z,n,'-b','LineWidth',1)
xlabel('\fontname{Times New Roman}Redshift (z)','FontSize',12)
ylabel('\fontname{Times New Roman}Log(n)','FontSize',12)
title('\fontname{Times New Roman} Number density against redshift (z)','FontSize',12)
set(gca,'xtick',0:1:5)
set(gca, 'XMinorTick','on', 'YMinorTick','on')
hold on
% Case 2: k=-1, Open
z = 0:0.0001:5;
% Defining constants
rho = 5*10^-27; % Upper density of the universe
c = 3*10^8;  % speed of light
kappa =-1; % Gives the value of k
R = 9*10^25; % cosmic scale factor, equal to value of R(to)
G = 6.67*10^-11; % Gravitational constant
N = 1; % Number of galaxies per unit volume
beta = 8*pi*G*c^-4; % Gives the value of beta
alpha = rho*R^3;
a = beta*c.^2*alpha-12*kappa*R;
b = ((beta*c.^2*alpha)*(1+z))-12*kappa*R;
n0 = 48*pi*N*R*(beta*c.^2*alpha).^2 *sqrt(3*R)*(sqrt(b)-sqrt(a)).^2;%numerator
d0 = (1+kappa*((sqrt(b)-sqrt(a))./(sqrt(a*b)+12*kappa*R)).^2).^3;
d1 = (sqrt(a*b)+12*kappa*R).^4;
d = d0.*d1; % Denominator
n=log(n0./d);
plot(z,n,'-g','LineWidth',1)
% Case 3: k=1, Closed
z = 0:0.0001:5;
% Defining constants
rho = 8.78*10^-25; % Upper density of the universe
c = 3*10^8;  % speed of light
kappa =1; % Gives the value of k
R = 9*10^25; % cosmic scale factor, equal to value of R(to)
G = 6.67*10^-11; % Gravitational constant
N = 1; % Number of galaxies per unit volume
beta = 8*pi*G*c^-4; % Gives the value of beta
alpha = rho*R^3;
a =(beta*c.^2*alpha)-12*kappa*R;
b =((beta*c.^2*alpha)*(1+z))-12*kappa*R;
n0 =48*pi*N*R*(beta*c.^2*alpha).^2 *sqrt(3*R)*(sqrt(b)-sqrt(a)).^2;%numerator
d0 =(1+kappa*((sqrt(b)-sqrt(a))./(sqrt(a*b)+12*kappa*R)).^2).^3;
d1 =(sqrt(a*b)+12*kappa*R).^4;
```

```
d = d0.*d1; % Denominator
n=log(n0./d);
plot(z,n,'-r','LineWidth',1.3)
legend('\rho=3 × 10^{−27}, \kappa= 0','\rho=5 × 10^{−27}, \kappa= −1 ','\rho= 8.78 ×
10^{−25}, \kappa= 1 ','Location','SouthEast')
% Modified model
% Case 1: k=0, Flat
z = 0:0.001:5;
% Defining constants
rho = 3*10^-27; % Upper density of the universe
c = 3*10^8;  % speed of light
kappa =0; % Gives the value of k
R = 9*10^25; % cosmic scale factor, equal to value of R(to)
G = 6.67*10^-11; % Gravitational constant
N = 1; % Number of galaxies per unit volume
epsilon = 0.45;
beta = 8*pi*G*c^-4; % Gives the value of beta
alpha = rho*R^3;
a1 =(beta*c.^2*alpha)-(12*kappa*R);
a2 =((beta*c^2*alpha)*(1+z./epsilon))-(12*kappa*R);
n0 =48*pi*N*R*(beta*c.^2*alpha).^2*sqrt(3*R)*(sqrt(a2)-sqrt(a1)).^2;%numerator
d0 =(1+kappa *((sqrt(a2)-sqrt(a1))./(sqrt(a1*a2)+12*kappa*R)).^2).^3;
d1 =(sqrt(a1*a2)+12*kappa*R).^4;
d = d1.*d0; % Denominator
n=log(n0./d);
plot(z,n,':b','LineWidth',1)
% Case 2: k=-1, Open
z = 0:0.001:5;
% Defining constants
rho = 5*10^-27; % Upper density of the universe
c = 3*10.^8;  % speed of light
kappa =-1; % Gives the value of k
R = 9*10^25; % cosmic scale factor, equal to value of R(to)
G = 6.67*10^-11; % Gravitational constant
N = 1; % Number of galaxies per unit volume
epsilon = 0.45;
beta = 8*pi*G*c^-4; % Gives the value of beta
alpha=rho*R^3;
a1 = (beta*c.^2*alpha)-12*kappa*R;
a2 = ((beta*c^2*alpha)*(1+z./epsilon))-(12*kappa*R);
n0 = 48*pi*N*R*(beta*c.^2*alpha).^2*sqrt(3*R)*(sqrt(a2)-sqrt(a1)).^2;%numerator
d0 = (1+kappa *((sqrt(a2)-sqrt(a1))./(sqrt(a1*a2)+12*kappa*R)).^2).^3;
d1 = (sqrt(a1*a2)+12*kappa*R).^4;
d = d1.*d0; % Denominator
n=log(n0./d);
plot(z,n,':g','LineWidth',1)
% Case 3: k=+1, Closed Universe = 0:0.001:5;
% Defining constants
rho = 8.78*10^-25; % Upper density of the universe
c = 3*10.^8;  % speed of light
kappa =1; % Gives the value of k
R = 9*10^25; % cosmic scale factor, equal to value of R(to)
G = 6.67*10^-11; % Gravitational constant
N = 1; % Number of galaxies per unit volume
epsilon = 0.45;
beta = 8*pi*G*c^-4; % Gives the value of beta
alpha = rho*R^3;
a1 =(beta*c.^2*alpha)-(12*kappa*R);
a2 =((beta*c^2*alpha)*(1+z./epsilon))-(12*kappa*R);
n0 =48*pi*N*R*(beta*c.^2*alpha).^2*sqrt(3*R)*(sqrt(a2)-sqrt(a1)).^2;%numerator
d0 =(1+kappa*((sqrt(a2)-sqrt(a1))./(sqrt(a1*a2)+12*kappa*R)).^2).^3;
d1 =(sqrt(a1*a2)+12*kappa*R).^4;
d = d1.*d0; % Denominator
n=log(n0./d);
plot(z,n,':r','LineWidth',1)
hold off
```